

1 Uribe-Convers and Tank: Diversification Linked to Biogeographic Movement

2

3

4

5

6

7

8 **Shifts in diversification rates linked to biogeographic movement into new areas: an**

9 **example of a recent radiation in the Andes<sup>1</sup>**

10

11

12 Simon Uribe-Convers<sup>2</sup> and David C. Tank

13 *Department of Biological Sciences, University of Idaho, 875 Perimeter MS 3051*

14 *Moscow, ID, 83844–3051, USA*

15

16

17

18

19

20

21

22

23

24 <sup>1</sup>Manuscript received \_\_\_\_\_; revision accepted \_\_\_\_\_.

25 <sup>2</sup>Author for correspondence: Simon Uribe-Convers; email: [uribe.convers@gmail.com](mailto:uribe.convers@gmail.com), web:

26 [www.simonuribe.com](http://www.simonuribe.com)

27

28 Acknowledgements

29 We would like to thank S. Mathews for kindly sharing genomic DNA for some taxa used in this

30 study. J. Sullivan, L. Harmon, E. Roalson, J. Beaulieu, B. Moore, N. Nürk, M. Pennell, T.

31 Peterson, and two anonymous reviewers for helpful suggestions or comments on the manuscript.

32 J. Beaulieu, L. Harmon, C. Blair and the University of Idaho Institute for Bioinformatics and

33 Evolutionary Studies (NIH/NCRR P20RR16448 and P20RR016454) for computational aid.

34 Funding for this work was provided by NSF DEB–[1210895](#) to DCT for SUC, NSF DEB–

35 [1253463](#) to DCT, and Graduate Student Research Grants to SUC from the Botanical Society of

36 America (BSA), the Society of Systematic Biologists (SSB), the American Society of Plant

37 Taxonomists (ASPT), and the University of Idaho Stillinger Herbarium Expedition Funds.

38

39

40

41

42

43

44

45

46

47 *Premise of the study:* Clade specific bursts in diversification are often associated with the  
48 evolution of key innovations. However, in groups with no obvious morphological innovations,  
49 observed upticks in diversification rates have also been attributed to the colonization of a new  
50 geographic environment. In this study, we explore the systematics, diversification dynamics, and  
51 historical biogeography of the plant clade Rhinanthaeae in the Orobanchaceae, with a special  
52 focus on the Andean clade of the genus *Bartsia* L..

53 *Methods:* We sampled taxa from across Rhinanthaeae, including a representative sample of  
54 Andean *Bartsia* species. Using standard phylogenetic methods, we reconstructed evolutionary  
55 relationships, inferred divergence times among the clades of Rhinanthaeae, elucidated their  
56 biogeographic history, and investigated diversification dynamics.

57 *Key results:* We confirmed that the South American *Bartsia* species form a highly supported  
58 monophyletic group. The median crown age of Rhinanthaeae was determined to be ca. 30 Ma, and  
59 Europe played an important role in the biogeographic history of the lineages. South America was  
60 first reconstructed in the biogeographic analyses around 9 Ma, and with a median age of 2.59  
61 Ma, this clade shows a significant uptick in diversification.

62 *Conclusions:* Increased net diversification of the South American clade corresponds with  
63 biogeographic movement into the New World. This happened at a time when the Andes were  
64 reaching the necessary elevation to host an alpine environment. Although a specific route could  
65 not be identified with certainty, we provide plausible hypotheses to how the group colonized the  
66 New World.

67 Keywords: *Bartsia*; *Bellardia*; Dispersification; Neobartsia; Orobanchaceae; Páramo;

68 Rhinanthaeae

69

70

71

72

73

74

75

76

77

78

79

80

81

82

83

84

85

86

87

88

89           The investigation of global patterns of biodiversity has a long history (e.g., Mittelbach et  
90 al., 2007). With the increase in our knowledge of phylogenetic relationships as well as methods  
91 for using phylogenies to understand diversification rates and biogeographic patterns (e.g., Ree et  
92 al., 2005; Alfaro et al., 2009), these global patterns can now be placed in an explicitly historical  
93 context (sensu Moore and Donoghue, 2007). Along these lines, differences in species richness  
94 between geographic areas have often been explained by climatic stability, age of the region,  
95 and/or niche conservatism that contributes to the slow, but steady, accumulation of species over  
96 time (Wiens and Donoghue, 2004). Likewise, clade specific bursts in net diversification  
97 (speciation minus extinction) are often associated with the evolution of novel morphologies,  
98 referred to as key innovations, such as nectar spurs in angiosperms (e.g., Hodges, 1997), molar  
99 characters in mammals (Woodburne et al., 2003), and feathers in birds (Ostrom, 1979). More  
100 recently, Moore and Donoghue (2007) demonstrated that in the plant families Adoxaceae and  
101 Valerianaceae, shifts in diversification rates were not correlated with the evolution of novel floral  
102 characters, but rather, with the movement into new geographic areas, and hypothesized that  
103 “dispersification” (dispersal and diversification) may play a larger role in shaping global  
104 biodiversity patterns than previously recognized. This is equivalent to the “key opportunity” of  
105 Donoghue and Sanderson (2015), and follows the hypothesis that in newly emerging  
106 environments, as long as the corridors for biogeographic movements are in place, these new  
107 areas will often be filled with lineages from environmentally similar areas where the relevant  
108 morphological and/or physiological adaptations are already in place (Donoghue, 2008).  
109 Empirical tests of these hypotheses not only require a robust estimate of phylogenetic  
110 relationships, but also the estimation of divergence times, diversification rates, and  
111 biogeographic patterns for the group of interest.

112           Various approaches have been taken to assess phylogenetic relationships, divergence  
113 times, and rates of diversification – each increasing our understanding of biodiversity and the  
114 way in which it has been produced. Bayesian analyses are now regularly used to estimate  
115 divergence times (e.g., Bacon et al., 2012; Drummond et al., 2012), most often performed in the  
116 program BEAST (Drummond and Rambaut, 2007), because the use of probabilistic priors  
117 accommodates both phylogenetic uncertainty (i.e., topology and branch lengths), as well as the  
118 timing of calibration points. Diversification rate analyses have been instrumental to our  
119 understanding of disparities in clade richnesses across the tree of life. For example, Alfaro et al.  
120 (2009) suggested that six pulses of accelerated diversification and three slowdowns, instead of  
121 single events, have shaped the current diversity of jawed vertebrates. Likewise, Tank et al.  
122 (2015) revealed a pattern of “nested radiations” across angiosperms—where clade-specific upticks  
123 in net diversification were nested within earlier diversification rate increases—and suggested that  
124 widely heterogeneous diversification rates have generated this pattern. Additionally, in the plant  
125 genus *Asclepias* L. (milkweeds) it has been shown that increases in the rate of diversification are  
126 tightly associated with the evolution of defense traits that prevent or minimize herbivory, and  
127 that this resulted in an adaptive radiation in the group (Agrawal et al., 2009). Moreover, studies  
128 of Andean plants, e.g., the family Valerianaceae (Bell and Donoghue, 2005a) and the genus  
129 *Lupinus* L. (Hughes and Eastwood, 2006; Drummond et al., 2012; Hughes and Atchison, 2015),  
130 have shown that groups with North American temperate ancestors have elevated diversification  
131 rates in the Andes, given that they were “pre-adapted” to the conditions of the newly and  
132 unoccupied niche at the time that they colonized the Andes (see also the ‘key landscape’ concept  
133 of Givnish [1997; 2015] to explain increased diversification rates in montane regions).

134 To investigate the influence of biogeographic movements on rates of diversification, we  
135 have chosen to study the mostly European clade Rhinanthaeae of the parasitic plant family  
136 Orobanchaceae (Wolfe et al., 2005; Bennett and Mathews, 2006; McNeal et al., 2013), with a  
137 particular focus on the genus *Bellardia* All., a clade of 48 species that are distributed across two  
138 disjunct geographic regions. The majority of the species in *Bellardia* were formerly part of the  
139 genus *Bartsia* L., which has been recently recircumscribed (Scheunert et al., 2012) to better  
140 reflect the evolutionary history of its species. Prior to this taxonomic rearrangement, *Bartsia* (49  
141 spp.) had two species distributed in the mountains of northeastern Africa (*B. decurva* Benth. and  
142 *B. longiflora* Benth.), one in the Mediterranean region (*B. trixago* L.), one in Scandinavia, the  
143 Alps, Greenland and the Hudson Bay region of northeastern North America (*B. alpina* L.), and  
144 the remaining 45 species distributed throughout the páramos of Andean South America (Molau,  
145 1990). Broad-scale phylogenetic studies of Orobanchaceae (Wolfe et al., 2005; Bennett and  
146 Mathews, 2006) and the Rhinanthaeae clade (Těšitel et al., 2010) had suggested that *Bartsia* was  
147 not monophyletic, but Scheunert et al. (2012) were the first to include species from the complete  
148 geographic distribution of the genus, as well as the two species of the related Mediterranean  
149 genus *Parentucellia* Viv.. However, because their sampling only included two species of the  
150 South American clade of *Bartsia*, they chose to only reclassify these two species, leaving ca. 43  
151 species in a large polyphyletic group with the monotypic lineage of *B. alpina* in Europe. The  
152 South American *Bartsia* species, which we will refer to here as the Neobartsia clade, are quite  
153 distinct from their Mediterranean counterparts (i.e., *Bellardia trixago*, and the two species of  
154 *Parentucellia* that were also moved to the expanded genus—*Bellardia latifolia* and *B. viscosa*) in  
155 multiple aspects. Ecologically, species in the Neobartsia clade grow at high elevation (ca. 3,000–  
156 5000 m) in wet environments while the Mediterranean species grow at low elevation (ca. 0–500

157 m) in seasonally dry environments. Geographically, the Neobartsia clade is restricted to the  
158 Andes while the Mediterranean taxa are native to the Mediterranean region and more recently  
159 have been introduced to Australia, coastal Chile, and coastal western North America. Finally, the  
160 Mediterranean species all have reflexed corolla lips, usually associated with bee pollination,  
161 whereas a large number of the species in the Neobartsia clade have erect corolla lips that are  
162 thought to be associated with hummingbird pollination due to their tubular shape and the  
163 placement of reproductive parts.

164 Previous studies of the group have only included a minor fraction of the South American  
165 species richness, usually sampling only one or two species, making it difficult to assess the  
166 influence of biogeographic movements on rates of diversification across the clade. Here, we  
167 included representatives from all clades (sensu Molau, 1990) comprising the former genus  
168 *Bartsia*, including a morphologically and geographically representative sampling of the South  
169 American diversity, as well as a representative sampling of all known allied genera of the  
170 Rhinanthae clade of Orobanchaceae, to establish a robust and well-supported phylogeny of the  
171 clade based on both chloroplast and nuclear ribosomal DNA sequence data. We then use this  
172 phylogeny to estimate divergence times across the clade and to investigate the biogeographic  
173 history of the clade, with a special focus on the origin of the Neobartsia clade in Andean South  
174 America. Finally, we use all these analyses to test if increases in rates of diversification are  
175 indeed associated with biogeographic movements into newly formed environments, i.e.,  
176 “dispersification” sensu Moore and Donoghue (2007).

177

178

179



180 MATERIALS AND METHODS

181 ***Sampling***—

182 A total of 49 taxa were included in this study (Table 1), with newly collected specimens  
183 stored in airtight plastic bags filled with silica gel desiccant in the field. Because our main focus  
184 is the diversification dynamics of the South American Neobartsia clade in the context of the  
185 disparate geographic distributions of the Old World species and the remainder of the mostly  
186 European Rhinanthae clade of Orobanchaceae, our sampling effort included representatives of  
187 10 of the 11 genera thought to comprise the clade (Wolfe et al., 2005; Bennett and Mathews,  
188 2006; Těšitel et al., 2010; Scheunert et al., 2012; McNeal et al., 2013). *Bellardia* and the  
189 Neobartsia clade are represented here by 15 South American species and two of the three  
190 Mediterranean taxa, *Bellardia trixago* (L.) All. and *Bellardia viscosa* (L.) Fisch. & C.A. Mey.  
191 The South American species were selected to encompass the morphological and geographic  
192 diversity in the clade. Based on previous results (Olmstead et al., 2001; Wolfe et al., 2005;  
193 Bennett and Mathews, 2006; Těšitel et al., 2010; Scheunert et al., 2012; McNeal et al., 2013)  
194 *Melampyrum* L. was used as the outgroup for the Rhinanthae clade.

195

196 ***Molecular Methods***—

197 Total genomic DNA was extracted from silica gel-dried tissue or herbarium material  
198 using a modified 2X CTAB method (Doyle and Doyle, 1987). Two chloroplast (cp) regions—  
199 *trnT-trnF* region and the *rps16* intron—were amplified via polymerase chain reaction (PCR)  
200 using the *trn-a* and *trn-f* (Taberlet et al., 1991) and the *rps16\_F* and *rps16\_R* primers (Oxelman  
201 et al., 1997), respectively. The nuclear ribosomal (nr) internal transcribed spacer (ITS) and  
202 external transcribed spacer (ETS) regions were amplified using the ITS4 and ITS5 primers

203 (Baldwin, 1992) and the ETS–B (Beardsley and Olmstead, 2002) and 18S–IGS (Baldwin and  
204 Markos, 1998), respectively. PCR profiles for all regions followed Tank and Olmstead (2008).  
205 When amplification of a region in one fragment was not possible, internal primers were used to  
206 amplify the region in multiple fragments. The primer pairs *trn-a/trnb*, *trnc/trn-d*, and *trn-e/trn-f*  
207 (Taberlet et al., 1991) were used to amplify the *trnT-trnF* region. Additionally, *Bellardia*  
208 specific internal primers were designed and used when these primer combinations failed  
209 (*trnT/trnL* intergenic spacer: *trnT-L\_iF* 5–CTTGGTTTTTCATCCGTAAAGG–3 and *trnT-L\_iR*  
210 5–CCTTTACGGATGAAAACCAAG–3). Following Tank and Olmstead (2008), the  
211 *rps16\_F/rps16\_iR* and *rps16\_iF/rps16\_2R* primer combinations were used to amplify the *rps16*  
212 intron in two fragments. Similarly, the ITS5/ITS2 and ITS3/ITS4 primer combinations (Baldwin,  
213 1992) were used to amplify the ITS region in two fragments.

214 PCR products were purified by precipitation in a 20% polyethylene glycol 8000  
215 (PEG)/2.5 M NaCl solution and washed in 70% ethanol prior to sequencing. To ensure accuracy,  
216 we sequenced both strands of the cleaned PCR products on an ABI 3130xl capillary DNA  
217 sequencer (Applied Biosystems, Foster City, California, USA) using ABI BigDye v.3.1 cycle  
218 sequencing chemistry. Sequence data were edited and assembled for each region using the  
219 program Sequencher v.4.7 (Gene Codes Corp., Ann Arbor, Michigan, USA), and consensus  
220 sequences were generated and submitted to GenBank (GenBank accessions: ETS: KM408174–  
221 KM408207, ITS: KM408208–KM408238, *trnT-trnL*: KM408239–KM408278, *rps16*:  
222 KM408279–KM408316, *trnL-trnF*: KM434082–KM434123). When sequencing was not  
223 possible for any given species or gene region, GenBank sequences were used to reduce the  
224 amount of missing data in the final matrix (Table 1).

225

226

227 ***Phylogenetic Analyses—***

228           Although two separate cpDNA regions were sequenced, the evolutionary histories of the  
229 *trnT-trnF* region and the *rps16* intron are tightly linked due to the nonrecombining nature of the  
230 chloroplast genome, and thus, were treated as a single locus. The nrDNA regions (ITS and ETS)  
231 were also treated as a single locus, given that they are linked because of their physical proximity  
232 in the nrDNA repeat. We created three primary datasets with our two independent loci: 1)  
233 cpDNA only, 2) nrDNA only, and 3) a combined cpDNA and nrDNA dataset. Given the wide  
234 phylogenetic diversity of sampled taxa, and relatively high molecular evolutionary rates of the  
235 nrDNA and cpDNA regions employed here, global alignments using default settings in Muscle  
236 v.3.6 contained many ambiguously aligned regions. Therefore, global alignments across the  
237 Rhinanthae clade were created for each gene region using the group-to-group profile alignment  
238 method as implemented in Muscle v.3.6 (Edgar, 2004). The group-to-group profile alignment  
239 method takes advantage of previous knowledge about monophyly of the major lineages (e.g.,  
240 Těšitel et al., 2010; Scheunert et al., 2012) and consists of lineage-specific alignments that are  
241 then iteratively aligned to one another resulting in fewer alignment ambiguities (Smith et al.,  
242 2009). These alignments were visually inspected and minor adjustments were made manually  
243 using Se-AL v.2.0a11 (Rambaut, 1996). Sites that could not be unambiguously aligned were  
244 excluded from the analyses. File format conversions and matrix concatenations were performed  
245 using the program Phyutility v.2.2 (Smith and Dunn, 2008).

246           A statistical selection of the best-fit model of nucleotide substitution according to the  
247 Akaike information criterion (AIC) was conducted independently for each gene region using the  
248 program jModelTest (Guindon and Gascuel, 2003; Posada, 2008). Based on these results,  
249 partitioned (by gene region) maximum likelihood (ML) analyses were performed on our three

250 primary datasets using RAxML v. 7.2.4 (Stamatakis, 2006) with 1,000 replicates of  
251 nonparametric bootstrapping using the rapid bootstrap algorithm (Stamatakis et al., 2008). Every  
252 fifth bootstrap tree generated by the rapid bootstrap analyses was used as a starting tree for full  
253 ML searches and the trees with the highest ML scores were chosen. Likewise, partitioned  
254 Bayesian inference (BI) analyses were performed using the parallel version of MrBayes v. 3.1.2  
255 (Ronquist and Huelsenbeck, 2003) with the individual parameters unlinked across the data  
256 partitions. Analyses consisted of two independent runs with four Markov chains using default  
257 priors and heating values. Each independent run consisted of 15 million generations and was  
258 started from a randomly generated tree and was sampled every 1,000 generations. Convergence  
259 of the chains was determined by analyzing the plots of all parameters and the  $-\ln L$  using Tracer  
260 v.1.5 (Rambaut and Drummond, 2004). Stationarity was assumed when all parameters values  
261 and the  $-\ln L$  had stabilized; the likelihoods of independent runs were considered  
262 indistinguishable when the average standard deviation of split frequencies was  $< 0.001$ .  
263 Consensus trees were obtained for each dataset using the `sumt` command in MrBayes. Finally,  
264 incongruences between the cpDNA and the nrDNA topologies were investigated using the  
265 approximately unbiased (AU) test (Shimodaira, 2002) and the Shimodaira–Hasegawa (SH) test  
266 (Shimodaira and Hasegawa, 1999), as implemented in the program CONSEL (Shimodaira and  
267 Hasegawa, 2001).

268

### 269 ***Divergence Time Estimation—***

270 To maximize the number of taxa in our dating analyses and to improve branch length  
271 estimation by minimizing the amount of missing data (Lemmon et al., 2009), we reduced our  
272 combined dataset to include sequences for only the cpDNA *trnT–trnL* intergenic spacer and the

273 nrDNA ITS region. This resulted in a dataset that included all 49 taxa and only 2% missing data,  
274 compared to 15% missing data for the complete dataset. Each gene was treated as a separate  
275 partition. To ensure convergence in divergence times, five independent runs were conducted  
276 using BEAST v.1.5.4 (Drummond and Rambaut, 2007). BEAST implements Markov Chain  
277 Monte Carlo (MCMC) methods that allow for uncertainty in both the topology and the  
278 calibration points, i.e., calibration points are treated as probabilistic priors, rather than point  
279 estimates (Ho and Phillips, 2009). It also implements an uncorrelated lognormal relaxed clock  
280 (UCLN) (Drummond et al., 2006), allowing every branch to have an independent substitution  
281 rate.

282         Each run was started from the resulting ML tree obtained for the dataset containing all  
283 regions, after performing a semiparametric rate smoothing based on penalized likelihood  
284 (Sanderson, 2002) in R (R Development Core Team, 2013) using the package Ape (Paradis et  
285 al., 2004). Each run consisted of 100,000,000 generations sampled every 1000 trees. The models  
286 of nucleotide substitution were kept unlinked for both partitions and the tree priors were kept as  
287 default under the birth–death process.

288         Because of the mostly herbaceous habit of the species in Orobanchaceae, there are no  
289 known fossils for the family. This lack of fossils made the dating of our analyses dependent on  
290 secondary calibrations obtained from a previous study. Based on explicit age estimates of an ITS  
291 molecular clock (Wolfe et al., 2005), a calibration point at the node containing every genus  
292 except *Melampyrum* (i.e., one node younger than the root) was used. This was done with a  
293 lognormal distribution prior with an offset of 25 million years (Ma), a mean of 0.9, and a  
294 standard deviation of 0.8, this way incorporating uncertainty in the calibration point. Because the  
295 use of this secondary calibration is far from ideal, to corroborate our calibration strategy, an

296 additional analysis using the most recent uplift of the Andes as the calibration point (Simpson,  
297 1975; Burnham and Graham, 1999; Gregory-Wodzicki, 2000; Antonelli et al., 2009) was  
298 conducted with a lognormal distribution prior (offset of 1.7 Myr, a mean of 0.2 and an standard  
299 deviation of 0.6). This calibration prior was set at the node where the species in the Neobartsia  
300 clade diverge from *B. viscosa*. This additional calibration scenario was conducted to assess the  
301 impact of alternative calibration points in the node ages.

302 Convergence of the parameters was monitored using Tracer v. 1.5 and the resulting trees  
303 were summarized using TreeAnnotator v.1.5.4 (Drummond and Rambaut, 2007) after 25% of the  
304 trees had been discarded as burn-in. Each of the five topologies and their node heights were  
305 visualized using FigTree v. 1.3.1 (Rambaut, 2006) and a final tree, representing the maximum  
306 clade credibility tree with information of the 95 percent highest posterior density (HPD), was  
307 obtained by combining the five runs using LogCombiner v.1.5.4 (Drummond and Rambaut,  
308 2007) and by summarizing them with TreeAnnotator v.1.5.4.

309

### 310 ***Biogeographic Analyses—***

311 The biogeographic history of *Bellardia* and allied genera was reconstructed using the  
312 program Lagrange v. C++ (Ree and Smith, 2008). Lagrange implements the maximum  
313 likelihood Dispersal–Extinction–Cladogenesis (DEC) model (Ree et al., 2005) to estimate the  
314 most likely ancestral geographic range based on current distributions of extant lineages. The  
315 DEC model has been used broadly to study biogeographic patterns in closely related taxa with  
316 restricted geographic areas (e.g., Fabre et al., 2013), large genera with cosmopolitan distributions  
317 (e.g., Emadzade et al., 2011), intercontinental migrations within families (e.g., Clayton et al.,  
318 2009), and large, diverse clades of angiosperms (e.g., Beaulieu et al., 2013). This model assumes

319 extinction or dispersal by contraction or expansion of the ancestral geographic range,  
320 respectively. Not only does Lagrange find the most likely ancestral area at a node, it calculates  
321 the probability of that area and compares it to other competing biogeographic scenarios. One of  
322 the caveats of this method, however, is that parameter space increases rapidly with the addition  
323 of geographic areas—it is currently advised to maintain the number of geographic areas for an  
324 unconstrained model to seven or eight. To alleviate this potential problem and introduce an  
325 additional advantage to biogeographic analyses, the user is given the option to assign a dispersal  
326 probability matrix based on prior knowledge of connectivity between areas, incorporating  
327 valuable ancestral geographic information. This is particularly important when proposed  
328 geographic areas are available only at certain time periods for various reasons—e.g., the  
329 formation or absence of a land bridge between continents, the uplift of a mountain, the formation  
330 of an island, etc.—which can result in more realistic dispersal routes. In plants however, most of  
331 this knowledge, at least for Northern Hemisphere temperate plants, is based on macrofossils of  
332 woody mesophytic taxa, e.g., *Quercus* (Tiffney and Manchester, 2001). Because the herbaceous  
333 genus *Bellardia* is almost completely restricted to alpine-like conditions that separate this  
334 lineage from the ecological conditions in which mesophytic forest species are found, and the vast  
335 majority of the Rhinanthae clade is also herbaceous, we consider that biological routes for these  
336 types of taxa are less well understood (Donoghue and Smith, 2004), and therefore, we did not  
337 include a dispersal probability matrix in our analyses (i.e., equal transition rates between all  
338 areas; see also Smith and Donoghue, 2010).

339 We used Lagrange on a posterior distribution of 1,000 randomly chosen trees (post burn-  
340 in) from our dating analyses. By inferring ancestral ranges over a posterior distribution of trees  
341 we are incorporating uncertainty in both topology as well as times of divergence (Smith, 2009;

342 Smith and Donoghue, 2010; Beaulieu et al., 2013). We conducted three independent analyses  
343 with varying distributions of current taxa. The first analysis was performed with conservative  
344 geographic ranges following Mabberley's Plant-Book (Mabberley, 2008), in which the genera  
345 have wider distributions, e.g., the genus *Euphrasia* L. has a north temperate distribution (Eurasia,  
346 Europe and Eastern North America). The second analysis included prior expert knowledge about  
347 the distribution of the genera based on published work, e.g., we followed the proposed Eurasian  
348 origin for the genus *Euphrasia* (Gussarova et al., 2008). The final analysis was based on species-  
349 specific distributions based on the explicit species that we sampled, i.e., species within a genus  
350 can have different distributions to account for endemisms and/or disparate distributions within a  
351 genus.

352 We considered species to be distributed in five distinct geographic areas: i) Eurasia  
353 (western Eurasia: the Balkan Peninsula and the Caucasus region), ii) Europe (including the  
354 Mediterranean climatic region in southern Europe and northern Africa), iii) Africa (montane  
355 northeastern Africa), iv) North America (Hudson Bay region of northeastern North America),  
356 and v) South America (including only the Andes). The results of the analyses were summarized  
357 in R. Following Beaulieu et al. (2013), we calculated Akaike weights for every biogeographic  
358 scenario reconstructed at every node in each tree separately. We then summed the Akaike  
359 weights for each node and averaged them across the distribution of trees, which resulted in  
360 composite Akaike weights ( $w_i$ ) for our biogeographic reconstructions. This means that the  
361 composite Akaike weights ( $w_i$ ) can be interpreted as being the relative likelihood of a given  
362 biogeographic scenario compared to other possible scenarios. Furthermore, we examined the  
363 evidence for the most supported scenario by calculating an evidence ratio of this model versus  
364 the next most supported model (Burnham and Anderson, 2002), i.e. the evidence ratio is the



365 relative likelihood of one model versus another ( $w_i/w_j$ ). These were interpreted as relative  
366 evidence of one scenario being the most supported when comparing it against competing  
367 biogeographic hypotheses (Beaulieu et al., 2013).

368

369

### 370 ***Diversification Rates***—

371 Diversification rate analyses were conducted on the same posterior distribution of 1,000  
372 trees, as well as on the maximum clade credibility (MCC) tree using MEDUSA (Alfaro et al.,  
373 2009), which is an extension of the method described by Rabosky et al. (2007) and is available in  
374 the R package geiger 2.0 (Pennell et al., 2014). In Rabosky et al. (2007), two likelihoods are  
375 estimated for a dated tree: i) a phylogenetic likelihood that uses the timing of the splits on the  
376 backbone to estimate ML values for birth and death rates following the equations of Nee et al.  
377 (1994), and ii) a taxonomic likelihood that uses species richness along with the date of the splits,  
378 estimating diversification rates following Magallón and Sanderson (2001). MEDUSA (Alfaro et  
379 al., 2009) looks for shifts in diversification rates in a stepwise manner by comparing AIC scores  
380 of successively more complex models. This method requires complete sampling that is achieved  
381 by collapsing clades of interest to a single tip and then assigning clade richnesses to these tip  
382 lineages. We collapsed our trees into tips representing each of the major lineages of Rhinanthaeae,  
383 which in most cases corresponded to each of the genera. The following clade richnesses were  
384 used: Neobartsia clade (45 spp.), *Parentucellia* clade (2 spp.), *Bellardia* clade (1 sp.), *Odontites*  
385 clade (32 spp.), *Euphrasia* clade (350 spp.), *Rhinanthus* clade (45 spp.), *Melampyrum* clade (35  
386 spp.), *Lathraea* clade (7 spp.), *Rhynchochrys orientalis* (1 spp.), *Rhynchochrys elephas* (1 spp.),  
387 *Rhynchochrys odontophylla* (1 spp.), *Rhynchochrys kurdica* (1 spp.), *Rhynchochrys stricta* (1

388 spp.), *Rhynchospora maxima* (1 spp.), *Bartsia alpina* (1 spp.), *Tozzia alpina* (1 spp.), *Hedbergia*  
389 *abyssinica* (1 spp.), *Hedbergia decurva* (1 spp.), *Hedbergia longiflora* (1 spp.).

390 To compare our MEDUSA results we conducted an additional analysis using the program  
391 SymmeTREE v1.0 (Chan and Moore, 2005). SymmeTREE is based on the topological  
392 distribution of species on the whole tree, which is compared to a distribution simulated on a tree  
393 under the equal-rates Markov random branching model (EMR), where the probability of a  
394 branching event is constant throughout the tree (Yule, 1924). If a clade shows an unbalanced  
395 distribution of species richness when compared to its sister clade, then a shift in the rate of  
396 diversification is identified. SymmeTREE also estimates several whole tree statistics that are  
397 evaluated against their own simulated null distribution, i.e., a constant pure-birth model (Chan  
398 and Moore, 2005). To accommodate topological and temporal uncertainty, we assessed  
399 diversification rate shifts with SymmeTREE using default settings across a random set of 542  
400 trees from the posterior distribution of trees from our divergence time analysis; the full set of  
401 1,000 trees was not used due to computational limitations.

402

## 403 RESULTS

### 404 *Molecular Methods*—

405 The cpDNA data set included the *trnT-trnF* region and the *rps16* intron and had a total  
406 length of 2,686 bp with 13% missing data. Similarly, the nrDNA dataset included the ITS and  
407 ETS regions with a total of 1,134 bp and 17% missing data. A combined data set was created  
408 from the cpDNA and the nrDNA matrices, with a total length of 3,820 bp and 15% missing data  
409 (files deposited in the Dryad Digital Repository: *data will be submitted after acceptance of the*  
410 *manuscript*).

411 ***Phylogenetic Analyses—***

412 Alignment of individual gene regions was straightforward requiring minor adjustments to  
413 the automated alignment strategy implemented in MUSCLE v. 3.6 (matrices and trees are  
414 available on TreeBase: *Temporary reviewer access*  
415 [http://purl.org/phylo/treebase/phylows/study/TB2:S11528?x-access-](http://purl.org/phylo/treebase/phylows/study/TB2:S11528?x-access-code=334b76effd95e3f56eb4ffe0185fc9ad&format=html)  
416 [code=334b76effd95e3f56eb4ffe0185fc9ad&format=html](http://purl.org/phylo/treebase/phylows/study/TB2:S11528?x-access-code=334b76effd95e3f56eb4ffe0185fc9ad&format=html)). Some regions that could not be  
417 unambiguously aligned in the *trnT-trnL* intergenic spacer and in the ETS region were excluded  
418 from the analyses (*trnT-L*: alignment positions 519–529 and 587–620; ETS: alignment positions  
419 63–65, 83–85 and 152–158). Model selection for the cpDNA regions yielded the General Time  
420 Reversible model +  $\Gamma$  (GTR) (Rodríguez et al., 1990) for the *trnT-trnF* intergenic spacer, and the  
421 Transversion model +  $\Gamma$  (TVM) for the *rps16* intron. The ITS and ETS regions resulted in the  
422 selection of the GTR+I+ $\Gamma$  and Hasegawa–Kishino–Yano+  $\Gamma$  (HKY) models, respectively. To  
423 avoid the difficulties of estimating  $\Gamma$  and the invariable sites simultaneously (Ronquist and  
424 Huelsenbeck, 2003; Yang, 2006), the model of substitution GTR+ $\Gamma$  with an increase in the  
425 number of rate categories from four to six was preferred in the case of the ITS region.

426 Our results from every dataset (Fig. 1 for the combined dataset and Fig. 2 for the cpDNA  
427 and nrDNA datasets) are in concordance with those presented in previous Rhinanthae studies  
428 (Těšitel et al., 2010; Scheunert et al., 2012), and assessment of incongruences between the  
429 cpDNA and nrDNA datasets showed that these were either not significant, or if they were, the  
430 alternative topology was only weakly supported. For example, the well-supported relationships  
431 in the cpDNA dataset between *Tozzia alpina* and *Hedbergia*—or between *Odontites* and  
432 *Bellardia*—are not statistically significant when constrained in the nrDNA dataset. Conversely,  
433 the relationship between *H. abyssinica* var. *nykiensis* and *H. decurva* found in the cpDNA

434 dataset is significant in the AU Test, but it is only moderately supported on the tree (BS 72, PP  
435 0.96) and it does not exist in the combined dataset (Table 2). An important new result from this  
436 study, which is based on the first widespread sampling of the group, is that the South American  
437 species indeed form a distinct clade, the Neobartsia clade, that is very well supported with a  
438 posterior probability (PP) of 1.0 and a bootstrap support (BS) of 100. *Bellardia*—including the  
439 Neobartsia clade—is sister to *Odontites* (PP 1.0, BS 92) and together are sister to a clade  
440 comprised by *Hedbergia* and *Tozzia alpina* (PP 1.0, BS 93). The placement of the genus *Tozzia*  
441 was uncertain until now, although the support of our analyses is marginal (PP 0.94, BS 80).  
442 Finally, the genus *Euphrasia* is sister to the latter genera (PP 1, BS 100) and together form a  
443 clade sister to *Bartsia alpina* (PP 1, BS 100). This last clade is what Scheunert et al. (2012)  
444 referred to as the core Rhinanthaeae.

445

#### 446 ***Divergence Time Estimation***—

447 When the calibration point was placed at the node where *Melampyrum* diverged from the  
448 remaining genera, the South American Neobartsia clade had a median age of 2.59 Ma (1.51–4.08  
449 Ma 95% HPD) (Table 3). The split between *Bellardia trixago* and the remaining species in the  
450 clade was estimated to have a median age of 8.73 Ma (5.12–12.76 Ma). The African clade  
451 diverged from *Tozzia alpina* 13.64 Ma (8.78–18.70 Ma), while the split of the European *Bartsia*  
452 *alpina* occurred 22.62 Ma (17.49–28.07 Ma). The root of the tree was estimated to have a  
453 median age of 30.65 Ma (25.55–38.83 Ma). Likewise, when the geological constraint was  
454 imposed, the Neobartsia clade had a median age of 2.63 Ma (1.97–3.58 Ma), and the divergence  
455 of *Bellardia trixago* from the remaining *Bellardia*–Neobartsia clade species occurred 8.48 Ma  
456 (4.95–12.48 Ma). The African clade diverged from *Tozzia alpina* 13.51 Ma (8.69–18.75 Ma),

457 *Bartsia alpina* of 22.33 Ma (16.23–28.36 Ma), and the root of the tree was estimated at 30.98 Ma  
458 (29.13–35.96 Ma). The age of the root is consistent with the date (35.5 Ma) inferred for this  
459 clade in an angiosperm wide analysis (Zanne et al., 2014). Because the results using different  
460 calibration strategies were within the 95 percent HPD of each other (see Table 3), we used the  
461 root calibration analysis for subsequent biogeographic and diversification rate analyses.

462

### 463 ***Biogeographic Analyses***—

464 Our three different codings of current geographic distribution resulted in very similar  
465 ancestral reconstructions (Table 4). Given that so much work has been done in recent years for  
466 several of these groups, e.g., *Bartsia/Bellardia* (Molau, 1990), *Euphrasia* (Gussarova et al.,  
467 2008), and *Odontites* (Bolliger, 1996), we favored the second coding scenario where current  
468 distributions were based on expert knowledge, including recent phylogenetic and biogeographic  
469 studies (for a wide-scale example on campanulids see Beaulieu et al., 2013). The most recent  
470 common ancestor (mrca) of the Rhinanthae clade of Orobanchaceae was likely distributed in  
471 Europe with a composite Akaike weight ( $w_i$ ) of 0.31 and an evidence ratio of 1.82 (Table 3).  
472 This ancestral range is maintained throughout the backbone of the tree until the node where  
473 *Euphrasia* diverges from the rest of the genera ( $w_i = 0.43$ , evidence ratio = 1.95). Nevertheless, a  
474 European ancestral range becomes the most supported reconstruction again at the node of  
475 divergence of *Odontites* ( $w_i = 0.80$ , evidence ratio = 8.88). A South American ancestral range is  
476 included for the first time at the crown node of *Bellardia*, where a  $w_i$  0.26 supports a split  
477 between Europe and South America and a  $w_i$  of 0.18 supports an entirely European ancestral  
478 range; the evidence ratio between these two reconstructions is 1.44. A Third scenario supporting  
479 a range comprised of Europe, Eurasia, and South America is supported by a  $w_i$  of 0.16; the

480 evidence ratio between this and the second most supported scenario is 1.13. The node where the  
481 Neobartsia clade diverges from the Mediterranean *Bellardia viscosa* is again supported by three  
482 competing models i) a split between Europe and South America ( $w_i=0.53$ , evidence ratio =  
483 1.51), ii) one between South America and an area comprised of Europe and Eurasia ( $w_i=0.35$ ,  
484 evidence ratio = 11.67), and iii) one containing Eurasia and South America ( $w_i=0.03$ ).  
485 Additional results for other genera can be seen on figure 3 and summarized in table 4.

486

487

#### 488 ***Diversification Rates***—

489 The rates reported in this study correspond to different parts of the tree, known as  
490 breakpoints (e.g., nodes, stems, or both) that are evolving under different parameter values, i.e.  
491 per-lineage net diversification and relative extinction rates (Pennell et al., 2014). Our analyses  
492 discovered six shifts in the rate of net diversification ( $r = \text{speciation} - \text{extinction}$ ) in the  
493 Rhinanthae clade when performed over the posterior distribution of trees; three of these were  
494 also identified on the MCC tree. Importantly, the three shifts identified on the MCC tree  
495 corresponded to the shifts that occurred at the highest frequency in the analyses across the  
496 posterior distribution of trees. Because most of these analyses were conducted on a posterior  
497 distribution of trees to incorporate phylogenetic uncertainty (both temporal and topological), we  
498 report the mean net diversification rate of each shift ( $r_{mean}$ ) in the text, and the ranges of these  
499 shifts in table 5. For the three shifts found in the MCC tree, we also report that value ( $r_{mcc}$ ). The  
500 first two shifts found in our analyses correspond to shifts that were only present in less than 15  
501 percent of the trees and show minimal deviation from the background rate of the tree. One of  
502 these shifts is on the node subtending the core Rhinanthae ( $r_{mean} = 0.11$ , frequency = 0.07) and  
503 the other one involves the hemiparasitic genus *Rhinanthus* L. and the holoparasite *Lathraea* L.

504 ( $r_{mean} = 0.17$ , frequency = 0.12). The latter shift could correspond to a change in life history from  
505 hemiparasitism to holoparasitism in *Lathraea*, but given the limited sampling of these two  
506 groups and the low frequency at which the shift was found we dare not comment further. The  
507 next shift involves a slowdown in the rate of *Bartsia alpina* ( $r_{mean} = -0.4$ ,  $r_{mcc} = 0$ ) and was the  
508 most frequent shift in the analyses (frequency = 1.17). The frequency higher than 1.0 for this  
509 node is an artifact of the way MEDUSA adds the shifts. When two sister clades each have a shift  
510 at their crown nodes, MEDUSA adds the parameters from both shifts and places the result on the  
511 stem leading to the two clades. Thus these shifts do not occur with a frequency higher than 1.0,  
512 but are very common. The fourth shift corresponds to an increase in net diversification ( $r_{mean} =$   
513 0.09) in the clade sister to *Bartsia alpina* and was found with a frequency of 0.32. An additional  
514 shift was found in the clade comprised of *Tozzia alpina* and the genus *Hedbergia*, the shift was  
515 found in 75% of the trees ( $r_{mean} = -0.06$ ;  $r_{mcc} = 0.05$ ). Finally, a shift showing an uptick in net  
516 diversification rate was present for the Neobartsia clade, with a frequency of 0.40 ( $r_{mean} = 0.40$ ;  
517  $r_{mcc} = 0.79$ ).

518 In comparison, the results obtained with SymmeTREE evidenced fewer diversification  
519 shifts on the whole tree ( $p < 0.05$ ). Like the MEDUSA results, an increase in diversification rate  
520 was also leading to the clade sister to *Bartsia alpina* and was consistently found in every tree we  
521 analyzed (Table 5). A shift showing a slowdown in the *Tozzia+Hedbergia* clade was found to be  
522 marginally significant at  $p < 0.05$  ( $p = 0.067$ ) in every tree. If we were to choose a less stringent  
523 significance threshold (e.g.,  $p < 0.10$ ), this shift would be significant in 506 trees (93% of the  
524 distribution). The same is true for the shift involving the Neobartsia clade, where it was only  
525 found to be significant in 77 trees at  $p < 0.05$  (14%), but increased to 258 trees (48%) when the  
526 less stringent  $p$  value was chosen.

527  
528  
529  
530  
531  
532  
533  
534  
535  
536  
537  
538  
539  
540  
541  
542  
543  
544  
545  
546  
547  
548  
549

## DISCUSSION

### *Systematic Implications*—

Molau (1990) published a comprehensive monograph on the genus “*Bartsia*”, where he hypothesized that the species formed a monophyletic group that was sister to the African monotypic genus *Hedbergia*. Our phylogenetic results (Figs. 1 and 2), which are in agreement with those of Těšitel et al. (2010) and Scheunert et al. (2012), show clearly that *Bartsia* sensu Molau is polyphyletic, and that the new classification (sensu Scheunert et al., 2012) better reflects the disparate geographic distributions of these lineages, as well as their evolutionary histories. Previous studies have recovered the basal relationships within *Bellardia* as a polytomy (Těšitel et al., 2010; Scheunert et al., 2012), where the position of *B. trixago*, *B. viscosa*, and *B. latifolia* is uncertain. Here, we recovered *Bellardia trixago* as sister to *B. viscosa* and the Neobartsia clade, but because we did not sample *B. latifolia*, we cannot be certain of the position of the other two taxa. The South American Neobartsia clade was highly supported in every analysis, and this is the first study to sample a geographically and morphologically representative diversity of the richness in this clade. These results provide strong evidence of the evolutionary distinctiveness of the Neobartsia clade with respect to the Mediterranean members of the expanded genus *Bellardia* (sensu Scheunert et al. 2012) – i.e., its unique geographic distribution and biogeographic history, the long divergence times from their Mediterranean relatives (~7.39 Ma), and the elevated diversification rates. Along with diagnostic morphological characters, we feel this justifies a reanalysis of the generic revision of Scheunert et al. (2012) with respect to the taxonomy in this clade, and this is the subject of ongoing taxonomic work in this clade.

Our cpDNA and nrDNA analyses placed the genus *Tozzia* in different positions in the tree, although these differences were not statistically significant (Table 2). Our combined



550 analysis placed the genus as sister to *Hedbergia*, albeit with marginal support (PP 0.94, BS 80).  
551 While this relationship is in agreement with previous studies (Těšitel et al., 2010; Scheunert et  
552 al., 2012), further work will be necessary to confidently place this genus in the Rhinanthaeae  
553 clade. Lastly, the African genus *Hedbergia* showed interesting and likely problematic species  
554 delimitations. The taxon *H. abyssinica* var. *nykiensis* was sister to *H. decurva* in our cpDNA  
555 analyses, and its relationship to the other *H. abyssinica* varieties in the nrDNA dataset was  
556 weakly supported. This is the first time that varietal taxa for this group have been included in a  
557 molecular study, and highlights the necessity for a more detailed study on the clade.

558

#### 559 ***Biogeography and Diversification Rates—***

560 Our divergence time and biogeographic results depicted in figure 3 illustrate evolutionary  
561 hypotheses regarding the current distribution of the Rhinanthaeae clade. As a reminder, our  
562 analyses were calibrated using dates obtained with the molecular rate of the ITS (Wolfe et al.,  
563 2005), and thus, they should be taken as estimates where some uncertainty is expected.  
564 Nevertheless, they provide an evolutionary foundation that helps explain the current distribution  
565 and the diversity of the South American Neobartsia clade. With no doubt, Europe played a major  
566 role, almost at every node, in the reconstruction of ancestral ranges in the Rhinanthaeae clade of  
567 Orobanchaceae. Although this is the first formal biogeographic analysis in the clade, these  
568 results are in line with the verbal biogeographic scenarios described in previous studies (Wolfe et  
569 al., 2005; Těšitel et al., 2010), but with slight differences in the description of the ancestral areas.  
570 Diversification of the majority of the genera was achieved in the European continent with  
571 subsequent migration events to Eurasia, northeastern North America, the Mediterranean region,  
572 Africa and South America. *Bartsia alpina* is a good example of a taxon with a purely European

573 ancestral distribution but that is currently distributed in other parts of the world. This suggests  
574 that the current distribution was the result of a second and more recent migration into Greenland  
575 and northeastern North America sometime along its very long branch (Fig. 3). *Odontites* is  
576 another good example of a European radiation that has expanded its range to include Eurasia  
577 after the initial divergence. Moreover, the genus *Euphrasia*, which accounts for more than half of  
578 the members of the clade with ~400 species, was reconstructed as having a Europe/Eurasian  
579 ancestral range. The few species sampled in this study all have Eurasian distributions but the  
580 genus is currently considered to have a “bipolar” distribution (Gussarova et al., 2008), with  
581 species distributed in north temperate regions and extreme Austral areas. This pattern is  
582 extremely interesting since it suggests that extinction and/or long distance dispersal have played  
583 a large role in shaping the current distribution of this large clade.

584         The Mediterranean region was not included as a distinct area in our reconstruction  
585 analyses, and therefore, some of the genera with current Mediterranean distributions were treated  
586 as European, e.g., *Rhynchocorys*, *Odontites*, *Bellardia trixago*, and *B. viscosa*. The  
587 Mediterranean climate, as recognized today, is a young environment formed only 2.3–3.2 Ma  
588 and it is the result of two main events: i) the establishment of the Mediterranean rhythm of dry  
589 summers and mild–cold winters ~3.2 Ma, and ii) the oldest xeric period know for the region ~2.2  
590 Ma (Zagwin, 1960; 1974; Suc, 1984). The crown clades for each of these genera were  
591 reconstructed to have a European ancestral distribution, which implies that their current ranges  
592 are the results of independent evolutions into the European Mediterranean climatic region not  
593 earlier than ~3.2 Ma.

594         This study is mainly focused on studying the diversity of the Neobartsia clade in the  
595 Andes, and to propose plausible hypotheses for its distribution. The Andes are thought to have

596 begun uplifting in the late Miocene (~10 Ma) but only reaching the necessary elevation to host  
597 alpine conditions in the late Pliocene or early Pleistocene 2–4 Ma (Simpson, 1975; Burnham and  
598 Graham, 1999; Gregory-Wodzicki, 2000; Antonelli et al., 2009). In our biogeographic analyses,  
599 South America is reconstructed for the first time at the crown node of *Bellardia*, with a median  
600 age of 8.73 Ma (5.12–12.76 Ma), and then at the node where *Bellardia viscosa* and the  
601 *Neobartsia* clade diverge (median age of 7.39 Ma [4.21–11.24 Ma]).  
602 These reconstructions, between 12.76 and 4.21 Ma, define an eight and a half million year  
603 window for the ancestor to have reached South America. There are two main land routes that  
604 were present during this time period, the North Atlantic Land Bridge (NALB) uniting  
605 northeastern North America and western Europe, and the Bering Land Bridge between eastern  
606 Asia and western North America. Previous studies in the plant family Malpighiaceae (Davis et  
607 al., 2002; 2004), have suggested a migration route from South America to Africa starting in the  
608 early Oligocene (~30 Ma) via North America, the NALB, and Europe. The NALB was available  
609 from the early Eocene (~50 Ma) until the middle to late Miocene (~10–8 Ma) (Tiffney, 1985;  
610 Tiffney and Manchester, 2001; Denk et al., 2010; 2011), dates which overlap with our  
611 divergence time estimates (Table 3) and with the appearance of South America as an ancestral  
612 range in our biogeographic analyses. This allows for the possibility of an early dispersal from  
613 Europe into North America over this land bridge. Colonization of North America would have  
614 followed a stepwise migration to South America over the forming Isthmus of Panama and/or  
615 island chains sometime in the last 4.5 Ma (Coates et al., 2004; Kirby and MacFadden, 2005;  
616 Retallack and Kirby, 2007). A caveat of this scenario is that it leaves a narrower window of time  
617 for a stepwise migration to have occurred. Moreover, the warmer temperatures in eastern North  
618 America during the late Miocene would possibly have affected the migration of a presumably

619 alpine adapted ancestor through the NALB.

620 An alternative stepwise migration scenario for the South American clade's colonization  
621 of the Andes involves a migration route through Beringia. This land bridge, which was available  
622 on-and-off from ~58–3.5 Ma (Hopkins, 1967; Tiffney and Manchester, 2001; Tiffney, 2008),  
623 has been proposed as a route for several groups found both in eastern Asia, western north  
624 America, and the Andes—e.g., Valerianaceae (Moore and Donoghue, 2007). The age of this land  
625 bridge overlaps completely with both the divergence of the Neobartsia clade from *Bellardia*  
626 *viscosa* (4.21–11.24 Ma), as well as with the split between *Bellardia trixago* and the other  
627 members of the *Bellardia*–Neobartsia clade 5.12–12.76 Ma. Moreover, this more recent route  
628 allows for the world to cool down during the Pliocene (Tiffney and Manchester, 2001), which  
629 may have facilitated the migration. This migration scenario is also plausible since Eurasia,  
630 Europe, and South America were reconstructed as the second most supported ancestral range at  
631 the node of divergence of the South American clade ( $w_i = 0.35$ ). Both of these stepwise migration  
632 scenarios rely completely on North America as an intermediary step where the South American  
633 ancestor possibly diversified, migrated, and finally went extinct. Unfortunately, there is no fossil  
634 record in the Rhinanthaeae clade (or in Orobanchaceae), and thus, no physical evidence is  
635 available to support either of these hypotheses.

636 Molau (1990) hypothesized that the Neobartsia clade had colonized the Andes via a  
637 long-distance dispersal from Africa, sometime in the early Pliocene (~5 Ma). This hypothesis  
638 seemed plausible at the time when no phylogenetic evidence was available for the clade, but now  
639 that it is clear that the former genus *Bartsia* is polyphyletic and the two African species  
640 (*Hebergia decurva*, *H. longifolia*) are not sister to the South American species, there is no longer  
641 support for this hypothesis. Nevertheless, there is a third hypothesis that does rely on long–

642 distance dispersal, but rather from Mediterranean Europe/north Africa to Andean South America  
643 (or, alternatively, from somewhere in North America following a land bridge migration from the  
644 Old World). Many plants are dispersed over long distances by water (e.g., *Cocos* L.), birds (e.g.,  
645 *Pisonia* L.), or wind (e.g., *Taraxacum* F.H. Wigg.), and physiological and morphological  
646 adaptations to float, adhere, or fly are common (reviewed in Howe and Smallwood, 1982). The  
647 seeds of *Bellarida*–*Neobartsia* clade are enclosed in a dry dehiscent capsule that contains  
648 between 20–200 small seeds (0.3–2 mm) per fruit, each equipped with 6–13 short wings or  
649 ridges (Molau, 1990). Although these seeds are light and have wings making them at first glance  
650 suitable for long distance traveling, it has been estimated that their mean dispersal distance is 0.3  
651 meters, at least in *Bartsia alpina* (Molau, 1990). The short mean dispersal distance is in strong  
652 disagreement with the distance that a seed would need to travel from the Mediterranean region to  
653 the New World (~7,000 km/~4,000 mi). Nevertheless, there is a known constant storm track  
654 from western Africa (including the northwestern African Mediterranean climatic region) that  
655 crosses the Atlantic Ocean into the Caribbean and the Americas, and recent evidence has shown  
656 that there are major influxes of African dust in southern North America (Bozlaker et al., 2013),  
657 northeastern South America (Prospero et al., 2014), and the Caribbean basin (Prospero and  
658 Mayol-Bracero, 2013). This opens the possibility for seeds of a Mediterranean ancestor to have  
659 been picked up and carried over to the New World. Although at first this may seem unlikely, it is  
660 important to point out that a single seed may be sufficient for the colonization of a new habitat,  
661 and that the eight and a half million year time window coupled with the large amounts (~200) of  
662 seeds that are produced in each capsule, increase the probability for this event to have happened.

663         At this point we cannot accept or reject any of the biogeographic hypotheses described  
664 above—the two stepwise migrations through North America or the long–distance dispersal from

665 the Mediterranean climatic region—and it highlights the difficulty of inferring ancestral  
666 colonization routes even when using modern ancestral range reconstruction methods (see Tripp  
667 and McDade, 2014), especially with a non-existent fossil record.

668 To investigate if these biogeographic movements have affected the rate at which clades  
669 are diversifying (i.e., “dispersification”), we need to assess if the shifts found in our analyses  
670 correlate with a movement into a new area or if there is something else, e.g., a morphological  
671 change, that has triggered them. Regardless of the reason, investigating shifts of diversification  
672 and the location of these on a phylogenetic tree is extremely helpful when trying to understand  
673 disparities in species richnesses across related clades. The comparison of two methods that are  
674 based on different tenets, a stepwise model testing approach vs. a topological imbalance  
675 approach (MEDUSA and SymmeTREE, respectively), allowed us to i) better evaluate the  
676 performance of different approaches used to identify shifts in diversification, while ii) making  
677 results shared by both methods robust and reliable. This comparison also showed the advantages  
678 of using a stepwise model testing approach and a method that incorporates extinction. Our  
679 MEDUSA analysis found six shifts across the posterior, and three when using the MCC tree; two  
680 of these six identified shifts represent a slowdown in net diversification. One of these  
681 slowdowns, which is the only shift consistently found by SymmeTREE at  $p < 0.01$ , across the  
682 posterior, and in the MCC tree, corresponds to the node where *Bartsia alpina* diverges from the  
683 rest of the core Rhinanthae 22.62 Ma. The extremely low diversification rate and its very long  
684 branch indicate that this species is likely the only extant member of a lineage that has had  
685 historically very low speciation rates or high extinction rates, or both. The first significant  
686 increase in net diversification rates was found at the node where the genus *Euphrasia* diverges  
687 from other genera 19.25 Ma. This genus includes ~400 species that encompass more than 80% of

688 the species richness of Rhinanthaeae, estimated to be ~528 spp. (Mabberley, 2008). Based on our  
689 limited sampling of this group, we cannot identify an apparent change in morphology or  
690 geography in the genus, and thus, no evident cause for this shift can be assessed with these data.  
691 Nevertheless, given the age and very high diversity of the clade, this shift is not surprising.  
692 However, it is important to point out that because we collapsed clades at the generic level to  
693 incorporate unsampled diversities, the present shift might not be the only one in *Euphrasia* and  
694 that clades within the genus may also have shifts of their own, where there might be an apparent  
695 change in either morphology or geography.

696 We also identified an increased rate of net diversification in the South American  
697 Neobartsia clade. We hypothesize that the clade underwent a similar pattern as seen in other  
698 Andean radiations, e.g. the family Valerianaceae and the genus *Lupinus* (Bell and Donoghue,  
699 2005b; Hughes and Eastwood, 2006, respectively), where their North American ancestor was  
700 “pre-adapted” to cold environments making the colonization of the high Andes, and further  
701 radiation, easier (Donoghue 2008). The Neobartsia clade has a median divergence time of 2.59  
702 Ma and a mean diversification rate of 0.40, however, when the analysis is performed on the  
703 MCC tree, the net diversification almost doubles ( $r_{mcc} = 0.79$ ). The large difference in values  
704 implies that although the shift was only identified in 40% of the posterior distribution of trees,  
705 when detected, the rate can be nearly four times higher than the background rate of the tree  
706 (background  $r_{mean} = 0.22$ ). Based on the very short branches within the clade, its young age, and  
707 the genetic similarity between the species included in this study, this shift likely resulted in a  
708 rapid radiation event where the movement to and colonization of the high Andes acted as a  
709 trigger to increased diversification. As the Andes were uplifting, the creation of alpine conditions  
710 promoted the radiation into the diversity that we see today. Accordingly, this is another

711 example of how the movement into a new geographic area, can lead to a high number of species  
712 in a relatively short period of time without the appearance of morphological key innovation,  
713 which is what Moore and Donoghue (2007) referred to as “dispersification”.

714

715 ***Conclusions—***

716 This study places the Neobartsia clade in the context of a robust and well-supported  
717 phylogeny within the Rhinanthaeae clade of Orobanchaceae. This is the first study to study this  
718 clade in an explicitly temporal framework, with detailed divergence time estimates for the clade.  
719 Here, we focused primarily on the colonization and diversification of Andean South America  
720 ~2.59 Ma. This date correlates well with the necessary age for the Andes to have acquired the  
721 adequate elevation to simulate alpine conditions for the establishment of this temperate, largely  
722 alpine clade in South America. Given that the South American clade is sister to a Mediterranean  
723 taxon, we hypothesized three biogeographic scenarios for the colonization of the Andes. The first  
724 route involves the NALB and North America as a stepwise migration route from Europe ~12–8  
725 Ma, whereas the second hypothesis involves a westerly route from Europe through Asia, the  
726 Bering Land Bridge, and North America ~12–4 Ma. Both of these scenarios share a second  
727 migration from North America to South America over the forming Isthmus of Panama and/or  
728 island chains in the mid to late Pliocene ~4.5–3.13 Ma, which gave rise to the Neobartsia clade,  
729 and high levels of extinction throughout Asia and/or North American. Finally, the third  
730 hypothesis involves a long-distance dispersal from the Mediterranean climatic region (Europe  
731 and northern Africa) to South America. At this point however, we cannot accept or reject any of  
732 the previously described hypotheses. Regardless of the biogeographic route taken, once the  
733 South American ancestor reached the Andes, it was able to diversify rapidly in the vacant niches



734 in the páramos. The greater diversification rates in the Neobartsia clade help explain the species  
735 richness found in the Andes today and support the idea that the “key opportunity” of geographic  
736 movement into a new area may trigger high diversification without the necessity of the evolution  
737 of morphological key innovations, and this may be especially true when the colonizing ancestral  
738 lineage is adapted to the new conditions it encounters.

739

740

#### LITERATURE CITED

- 741 AGRAWAL, A.A., M. FISHBEIN, R. HALITSCHKE, A.P. HASTINGS, D.L. RABOSKY, AND S.  
742 RASMANN. 2009. Evidence for adaptive radiation from a phylogenetic study of plant  
743 defenses. *Proceedings of the National Academy of Sciences* 106: 18067–18072.
- 744 ALFARO, M.E., F. SANTINI, C. BROCK, H. ALAMILLO, A. DORNBURG, D. RABOSKY, G.  
745 CARNEVALE, AND L. HARMON. 2009. Nine exceptional radiations plus high turnover explain  
746 species diversity in jawed vertebrates. *Proceedings of the National Academy of Sciences*  
747 106: 13410.
- 748 ANTONELLI, A., J.A.A. NYLANDER, C. PERSSON, AND I. SANMARTÍN. 2009. Tracing the impact of  
749 the Andean uplift on Neotropical plant evolution. *Proceedings of the National Academy of*  
750 *Sciences* 106: 9749–9754.
- 751 BACON, C.D., W.J. BAKER, AND M.P. SIMMONS. 2012. Miocene Dispersal Drives Island  
752 Radiations in the Palm Tribe Trachycarpeae (Arecaceae). *Systematic Biology* 61: 426–442.
- 753 BALDWIN, B.G. 1992. Phylogenetic Utility of the Internal Transcribed Spacers of Nuclear  
754 Ribosomal DNA in Plants: An Example from the Compositae. *Molecular phylogenetics and*  
755 *evolution* 1: 3–16.
- 756 BALDWIN, B.G., AND S. MARKOS. 1998. Phylogenetic Utility of the External Transcribed Spacer  
757 (ETS) of 18S–26S rDNA: Congruence of ETS and ITS Trees of *Calycadenia* (Compositae).  
758 *Molecular phylogenetics and evolution* 10: 449–463.
- 759 BEARDSLEY, P.M., AND R.G. OLMSTEAD. 2002. Redefining Phrymaceae: the placement of  
760 *Mimulus*, tribe Mimuleae, and *Phryma*. *American Journal of Botany* 89: 1093–1102.
- 761 BEAULIEU, J.M., D.C. TANK, AND M.J. DONOGHUE. 2013. A Southern Hemisphere origin for  
762 campanulid angiosperms, with traces of the break-up of Gondwana. *BMC Evolutionary*  
763 *Biology* 13: 80.
- 764 BELL, C., AND M. DONOGHUE. 2005a. Phylogeny and biogeography of Valerianaceae  
765 (Dipsacales) with special reference to the South American valerians. *Organisms Diversity &*  
766 *Evolution* 5: 147–159.

- 767 BELL, C., AND M. DONOGHUE. 2005b. Dating the Dipsacales: comparing models, genes, and  
768 evolutionary implications. *American Journal of Botany* 92: 284.
- 769 BENNETT, J.R., AND S. MATHEWS. 2006. Phylogeny of the parasitic plant family Orobanchaceae  
770 inferred from phytochrome A. *American Journal of Botany* 93: 1039–1051.
- 771 BOLLIGER, M. 1996. Monographie der Gattung *Odontites* (Scrophulariaceae) sowie der  
772 verwandten Gattungen *Macrosyringion*, *Odontitella*, *Bornmuellerantha* und *Bartsiella*.  
773 *Willdenowia* 26: 37–168.
- 774 BOZLAKER, A., J.M. PROSPERO, M.P. FRASER, AND S. CHELLAM. 2013. Quantifying the  
775 contribution of long-range Saharan dust transport on particulate matter concentrations in  
776 Houston, Texas, using detailed elemental analysis. *Environmental science & technology* 47:  
777 10179–10187.
- 778 BURNHAM, K.P., AND D.R. ANDERSON. 2002. Model selection and multi-model inference: a  
779 practical information-theoretic approach. Second Edition. Springer New York, New York.
- 780 BURNHAM, R.J., AND A. GRAHAM. 1999. The history of neotropical vegetation: new  
781 developments and status. *Annals of the Missouri Botanical Garden* 546–589.
- 782 CHAN, K., AND B. MOORE. 2005. SymmeTREE: whole-tree analysis of differential  
783 diversification rates. *Bioinformatics* 21: 1709.
- 784 CLAYTON, J.W., P.S. SOLTIS, AND D.E. SOLTIS. 2009. Recent Long-Distance Dispersal  
785 Overshadows Ancient Biogeographical Patterns in a Pantropical Angiosperm Family  
786 (Simaroubaceae, Sapindales). *Systematic Biology* 58: 395–410.
- 787 COATES, A., L. COLLINS, M. AUBRY, AND W. BERGGREN. 2004. The geology of the Darien,  
788 Panama, and the late Miocene-Pliocene collision of the Panama arc with northwestern South  
789 America. *Geological Society of America Bulletin* 116: 1327.
- 790 DAVIS, C.C., C.D. BELL, S. MATHEWS, AND M.J. DONOGHUE. 2002. Laurasian migration explains  
791 Gondwanan disjunctions: evidence from Malpighiaceae. *Proceedings of the National  
792 Academy of Sciences of the United States of America* 99: 6833–6837.
- 793 DAVIS, C.C., P.W. FRITSCH, C.D. BELL, AND S. MATHEWS. 2004. High-latitude Tertiary  
794 migrations of an exclusively tropical clade: evidence from Malpighiaceae. *International  
795 Journal of Plant Sciences* 165: S107–S121.
- 796 DENK, T., F. GRIMSSON, AND R. ZETTER. 2010. Episodic migration of oaks to Iceland: Evidence  
797 for a North Atlantic “land bridge” in the latest Miocene. *American Journal of Botany* 97:  
798 276–287.
- 799 DENK, T., F. GRÍMSSON, R. ZETTER, AND L.A. SÍMONARSON. 2011. The Biogeographic History of  
800 Iceland – The North Atlantic Land Bridge Revisited. In *Topics in Geobiology, Topics in  
801 Geobiology*, 647–668. Springer Netherlands, Dordrecht.

- 802 DONOGHUE, M., AND S. SMITH. 2004. Patterns in the assembly of temperate forests around the  
803 Northern Hemisphere. *Philosophical Transactions B* 359: 1633.
- 804 DONOGHUE, M.J. 2008. A phylogenetic perspective on the distribution of plant diversity.  
805 *Proceedings of the National Academy of Sciences of the United States of America* 105:  
806 11549–11555.
- 807 DONOGHUE, M.J., AND M.J. SANDERSON. 2015. Confluence, synnovation, and depauperons in  
808 plant diversification. *New Phytologist* 207: 260–274.
- 809 DOYLE, J.J., AND J.L. DOYLE. 1987. A rapid DNA isolation procedure for small quantities of  
810 fresh leaf tissue. *Phytochemical Bulletin* 19: 11–15.
- 811 DRUMMOND, A., AND A. RAMBAUT. 2007. BEAST: Bayesian evolutionary analysis by sampling  
812 trees. *BMC Evolutionary Biology* 7: 214.
- 813 DRUMMOND, A., S. HO, M. PHILLIPS, AND A. RAMBAUT. 2006. Relaxed phylogenetics and dating  
814 with confidence. *PLoS Biology* 4: 699.
- 815 DRUMMOND, C.S., R.J. EASTWOOD, S.T.S. MIOTTO, AND C.E. HUGHES. 2012. Multiple  
816 continental radiations and correlates of diversification in *Lupinus* (Leguminosae): testing for  
817 key innovation with incomplete taxon sampling. *Systematic Biology* 61: 443–460.
- 818 EDGAR, R.C. 2004. MUSCLE: multiple sequence alignment with high accuracy and high  
819 throughput. *Nucleic Acids Research* 32: 1792–1797.
- 820 EMADZADE, K., B. GEHRKE, H.P. LINDER, AND E. HÖRANDL. 2011. The biogeographical history  
821 of the cosmopolitan genus *Ranunculus* L. (Ranunculaceae) in the temperate to meridional  
822 zones. *Molecular phylogenetics and evolution* 58: 4–21.
- 823 FABRE, P.-H., M. MOLTENSEN, J. FJELDSA, M. IRESTEDT, J.-P. LESSARD, AND K.A. JØNSSON.  
824 2013. Multiple waves of colonization by monarch flycatchers (*Myiagra*, Monarchidae)  
825 across the Indo-Pacific and their implications for coexistence and speciation. *Journal of*  
826 *Biogeography* 41: 274–286.
- 827 GIVNISH, T.J. 1997. Adaptive radiation and molecular systematics: issues and approaches. Pp:  
828 1-54 in: T.J. Givnish and K.J. Systma, eds. *Molecular Evolution and Adaptive Radiation*.  
829 Cambridge University Press, Cambridge.
- 830 GIVNISH, T.J. 2015. Adaptive radiation versus ‘radiation’ and ‘explosive diversification’: why  
831 conceptual distinctions are fundamental to understanding evolution. *New Phytologist* 207:  
832 297–303.
- 833 GREGORY-WODZICKI, K. 2000. Uplift history of the Central and Northern Andes: a review.  
834 *Geological Society of America Bulletin* 112: 1091.
- 835 GUINDON, S., AND O. GASCUEL. 2003. A simple, fast, and accurate algorithm to estimate large  
836 phylogenies by maximum likelihood. *Systematic Biology* 52: 696–704.

- 837 GUSSAROVA, G., M. POPP, E. VITEK, AND C. BROCHMANN. 2008. Molecular phylogeny and  
838 biogeography of the bipolar *Euphrasia* (Orobanchaceae): recent radiations in an old genus.  
839 *Molecular phylogenetics and evolution* 48: 444–460.
- 840 HO, S., AND M. PHILLIPS. 2009. Accounting for Calibration Uncertainty in Phylogenetic  
841 Estimation of Evolutionary Divergence Times. *Systematic Biology* 58: 367–380.
- 842 HODGES, S.A. 1997. Floral Nectar Spurs and Diversification. *International Journal of Plant*  
843 *Sciences* 158: S81–S88.
- 844 HOPKINS, D.M. 1967. The Bering land bridge. Stanford University Press, Stanfor, CA.
- 845 HOWE, H.F., AND J. SMALLWOOD. 1982. Ecology of Seed Dispersal. *Annual Review of Ecology*  
846 *and Systematics* 13: 201–228.
- 847 HUGHES, C., AND R. EASTWOOD. 2006. Island radiation on a continental scale: exceptional rates  
848 of plant diversification after uplift of the Andes. *Proceedings of the National Academy of*  
849 *Sciences* 103: 10334.
- 850 HUGHES, C.E., AND G.W. ATCHISON. 2015. The ubiquity of alpine plant radiations: from the  
851 Andes to the Hengduan Mountains. *New Phytologist* 207: 275–282.
- 852 KIRBY, M.X., AND B. MACFADDEN. 2005. Was southern Central America an archipelago or a  
853 peninsula in the middle Miocene? A test using land-mammal body size. *Palaeogeography,*  
854 *palaeoclimatology, palaeoecology* 228: 193–202.
- 855 LEMMON, A.R., J.M. BROWN, K. STANGER-HALL, AND E.M. LEMMON. 2009. The effect of  
856 ambiguous data on phylogenetic estimates obtained by maximum likelihood and Bayesian  
857 inference. *Systematic Biology* 58: 130–145.
- 858 MABBERLEY, D.J. 2008. Mabblerley’s plant-book: a portable dictionary of plants, their  
859 classification and uses. 3rd ed. Cambridge, UK. University Press.
- 860 MAGALLÓN, S., AND M.J. SANDERSON. 2001. Absolute diversification rates in angiosperm clades.  
861 *Evolution* 55: 1762–1780.
- 862 MCNEAL, J.R., J.R. BENNETT, A.D. WOLFE, AND S. MATHEWS. 2013. Phylogeny and origins of  
863 holoparasitism in Orobanchaceae. *American Journal of Botany* 100: 971–983.
- 864 MITTELBACH, G.G., D.W. SCHEMSKE, H.V. CORNELL, A.P. ALLEN, J.M. BROWN, M.B. BUSH,  
865 S.P. HARRISON, ET AL. 2007. Evolution and the latitudinal diversity gradient: speciation,  
866 extinction and biogeography. *Ecology Letters* 10: 315–331.
- 867 MOLAU, U. 1990. The genus *Bartsia* (Scrophulariaceae - Rhinanthoideae ). *Opera Botanica* 102:  
868 1–100.
- 869 MOORE, B.R., AND M.J. DONOGHUE. 2007. Correlates of diversification in the plant clade  
870 Dipsacales: geographic movement and evolutionary innovations. *The American Naturalist*

- 871 170 Suppl 2: S28–55.
- 872 NEE, S., R.M. MAY, AND P.H. HARVEY. 1994. The reconstructed evolutionary process.  
873 *Philosophical transactions of the Royal Society of London. Series B, Biological sciences*  
874 344: 305–311.
- 875 OLMSTEAD, R.G., C.W. DEPAMPHILIS, A.D. WOLFE, N.D. YOUNG, W.J. ELISONS, AND P.A.  
876 REEVES. 2001. Disintegration of the Scrophulariaceae. *American Journal of Botany* 88: 348–  
877 361.
- 878 OSTROM, J.H. 1979. Bird flight: how did it begin? *American Scientist* 67: 46–56.
- 879 OXELMAN, B., M. LIDÉN, AND D. BERGLUND. 1997. Chloroplast rps16 intron phylogeny of the  
880 tribe Sileneae (Caryophyllaceae). *Plant Systematics and Evolution* 206: 393–410.
- 881 PARADIS, E., J. CLAUDE, AND K. STRIMMER. 2004. APE: Analyses of Phylogenetics and  
882 Evolution in R language. *Bioinformatics* 20: 289–290.
- 883 PENNELL, M.W., J.M. EASTMAN, G.J. SLATER, J.W. BROWN, J.C. UYEDA, R.G. FITZJOHN, M.E.  
884 ALFARO, AND L.J. HARMON. 2014. geiger v2.0: an expanded suite of methods for fitting  
885 macroevolutionary models to phylogenetic trees. *Bioinformatics* 30: 2216–2218.
- 886 POSADA, D. 2008. jModelTest: phylogenetic model averaging. *Molecular Biology and Evolution*  
887 25: 1253–1256.
- 888 PROSPERO, J.M., AND O.L. MAYOL-BRACERO. 2013. Understanding the Transport and Impact of  
889 African Dust on the Caribbean Basin. *Bulletin of the American Meteorological Society* 94:  
890 1329–1337.
- 891 PROSPERO, J.M., F.X. COLLARD, J. MOLINIÉ, AND A. JEANNOT. 2014. Characterizing the annual  
892 cycle of African dust transport to the Caribbean Basin and South America and its impact on  
893 the environment and air quality. *Global Biogeochemical Cycles* 29:.
- 894 R DEVELOPMENT CORE TEAM. 2013. R: A language and environment for statistical computing. R  
895 *Foundation for Statistical Computing, Vienna, Austria. ISBN 3-900051-07-0, URL*  
896 <http://www.R-project.org>.
- 897 RABOSKY, D.L., S.C. DONNELLAN, A.L. TALABA, AND I.J. LOVETTE. 2007. Exceptional among-  
898 lineage variation in diversification rates during the radiation of Australia's most diverse  
899 vertebrate clade. *Proceedings of the Royal Society B: Biological Sciences* 274: 2915–2923.
- 900 RAMBAUT, A. 2006. FigTree. *Institute of Evolutionary Biology, University of Edinburgh,*  
901 *Edinburgh, UK. Available at <http://tree.bio.ed.ac.uk/software/figtree/>.*
- 902 RAMBAUT, A. 1996. Se-AL: Sequence alignment editor. *Institute of Evolutionary Biology,*  
903 *University of Edinburgh, Edinburgh, UK. Available at <http://tree.bio.ed.ac.uk/software/seal/>.*
- 904 RAMBAUT, A., AND A.J. DRUMMOND. 2004. Tracer. *University of Edinburgh, Edinburgh, UK.*



- 905 Available at <http://tree.bio.ed.ac.uk/software/tracer/>.
- 906 REE, R., B. MOORE, C. WEBB, AND M. DONOGHUE. 2005. A likelihood framework for inferring  
907 the evolution of geographic range on phylogenetic trees. *Evolution* 59: 2299–2311.
- 908 REE, R.H., AND S.A. SMITH. 2008. Maximum likelihood inference of geographic range evolution  
909 by dispersal, local extinction, and cladogenesis. *Systematic Biology* 57: 4–14.
- 910 RETALLACK, G., AND M. KIRBY. 2007. Middle Miocene global change and paleogeography of  
911 Panama. *Palaios* 22: 667–679.
- 912 RODRÍGUEZ, F., J.L. OLIVER, A. MARÍN, AND J.R. MEDINA. 1990. The general stochastic model  
913 of nucleotide substitution. *Journal of theoretical biology* 142: 485–501.
- 914 RONQUIST, F., AND J.P. HUELSENBECK. 2003. MrBayes 3: Bayesian phylogenetic inference under  
915 mixed models. *Bioinformatics* 19: 1572–1574.
- 916 SANDERSON, M.J. 2002. Estimating absolute rates of molecular evolution and divergence times: a  
917 penalized likelihood approach. *Molecular Biology and Evolution* 19: 101–109.
- 918 SCHEUNERT, A., A. FLEISCHMANN, C. OLANO-MARIN, C. BRÄUCHLER, AND G. HEUBL. 2012.  
919 Phylogeny of tribe Rhinanthae (Orobanchaceae) with a focus on biogeography, cytology  
920 and re-examination of generic concepts. *Taxon* 61: 1269–1285.
- 921 SHIMODAIRA, H. 2002. An approximately unbiased test of phylogenetic tree selection. *Systematic  
922 Biology* 51: 492–508.
- 923 SHIMODAIRA, H., AND M. HASEGAWA. 2001. CONSEL: for assessing the confidence of  
924 phylogenetic tree selection. *Bioinformatics* 17: 1246–1247.
- 925 SHIMODAIRA, H., AND M. HASEGAWA. 1999. Multiple comparisons of log-likelihoods with  
926 applications to phylogenetic inference. *Molecular Biology and Evolution* 16: 1114.
- 927 SIMPSON, B. 1975. Pleistocene changes in the flora of the high tropical Andes. *Paleobiology*  
928 273–294.
- 929 SMITH, S. 2009. Taking into account phylogenetic and divergence-time uncertainty in a  
930 parametric biogeographical analysis of the Northern Hemisphere plant clade Caprifoliaceae.  
931 *Journal of Biogeography* 36: 2324–2337.
- 932 SMITH, S., AND C. DUNN. 2008. Phyutility: a phyloinformatics tool for trees, alignments and  
933 molecular data. *Bioinformatics* 24: 715.
- 934 SMITH, S.A., AND M.J. DONOGHUE. 2010. Combining historical biogeography with niche  
935 modeling in the *Caprifolium* clade of *Lonicera* (Caprifoliaceae, Dipsacales). *Systematic  
936 Biology* 59: 322–341.
- 937 SMITH, S.A., J.M. BEAULIEU, AND M.J. DONOGHUE. 2009. Mega-phylogeny approach for

- 938 comparative biology: an alternative to supertree and supermatrix approaches. *BMC*  
939 *Evolutionary Biology* 9: 37.
- 940 STAMATAKIS, A. 2006. RAxML-VI-HPC: maximum likelihood-based phylogenetic analyses  
941 with thousands of taxa and mixed models. *Bioinformatics* 22: 2688–2690.
- 942 STAMATAKIS, A., P. HOOVER, AND J. ROUGEMONT. 2008. A Rapid Bootstrap Algorithm for the  
943 RAxML Web Servers. *Systematic Biology* 57: 758–771.
- 944 SUC, J.P. 1984. Origin and evolution of the Mediterranean vegetation and climate in Europe.  
945 *Nature* 307: 429–432.
- 946 TABERLET, P., L. GIELLY, G. PAUTOU, AND J. BOUVET. 1991. Universal primers for amplification  
947 of three non-coding regions of chloroplast DNA. *Plant Molecular Biology* 17: 1105–1109.
- 948 TANK, D., AND R. OLMSTEAD. 2008. From annuals to perennials: phylogeny of subtribe  
949 Castillejinae (Orobanchaceae). *American Journal of Botany* 95: 608–625.
- 950 TANK, D.C., J.M. EASTMAN, M.W. PENNELL, P.S. SOLTIS, D.E. SOLTIS, C.E. HINCHLIFF, J.W.  
951 BROWN, ET AL. 2015. Nested radiations and the pulse of angiosperm diversification:  
952 increased diversification rates often follow whole genome duplications. *New Phytologist*  
953 207: 454–467.
- 954 TĚŠITEL, J., P. ŘÍHA, Š. SVOBODOVÁ, T. MALINOVÁ, AND M. ŠTECH. 2010. Phylogeny, Life  
955 History Evolution and Biogeography of the Rhinanthoid Orobanchaceae. *Folia Geobotanica*  
956 45: 347–367.
- 957 TIFFNEY, B., AND S. MANCHESTER. 2001. The use of geological and paleontological evidence in  
958 evaluating plant phylogeographic hypotheses in the Northern Hemisphere Tertiary.  
959 *International Journal of Plant Sciences* 162: 3–17.
- 960 TIFFNEY, B.H. 1985. Perspectives on the origin of the floristic similarity between eastern Asia  
961 and eastern North America. *Journal of the Arnold Arboretum* 66: 73–94.
- 962 TIFFNEY, B.H. 2008. Phylogeography, fossils, and northern hemisphere biogeography: the role of  
963 physiological uniformitarianism. *Annals of the Missouri Botanical Garden* 95: 135–143.
- 964 TRIPP, E.A., AND L.A. MCDADE. 2014. A rich fossil record yields calibrated phylogeny for  
965 Acanthaceae (Lamiales) and evidence for marked biases in timing and directionality of  
966 intercontinental disjunctions. *Systematic Biology* 63: 660–684.
- 967 WIENS, J.J., AND M.J. DONOGHUE. 2004. Historical biogeography, ecology and species richness.  
968 *Trends in Ecology & Evolution* 19: 639–644.
- 969 WOLFE, A., C. RANDLE, L. LIU, AND K. STEINER. 2005. Phylogeny and biogeography of  
970 Orobanchaceae. *Folia Geobotanica* 40: 115–134.
- 971 WOODBURN, M.O., T.H. RICH, AND M.S. SPRINGER. 2003. The evolution of tribospheny and the

- 972           antiquity of mammalian clades. *Molecular phylogenetics and evolution* 28: 360–385.
- 973    YANG, Z. 2006. Computational Molecular Evolution. Oxford University Press.
- 974    YULE, G.U. 1924. A mathematical theory of evolution, based on the conclusions of Dr. J. C.  
975           Willis, F.R.S. *Philosophical Transactions of the Royal Society B: Biological Sciences* 213:  
976           21–87.
- 977    ZAGWIN, W.H. 1960. Aspects of the Pliocene and early Pleistocene vegetation and climate in the  
978           Netherlands. *Mededelingen Geologische Strichting* 3: 1–78.
- 979    ZAGWIN, W.H. 1974. The Pliocene-Pleistocene boundary in western and southern Europe.  
980           *Boreas* 3: 75–97.
- 981    ZANNE, A.E., D.C. TANK, W.K. CORNWELL, J.M. EASTMAN, S.A. SMITH, R.G. FITZJOHN, D.J.  
982           MCGLINN, ET AL. 2014. Three keys to the radiation of angiosperms into freezing  
983           environments. *Nature* 506: 89–92.
- 984
- 985
- 986



Table 1. Taxa and voucher information for plant material from which DNA was extracted. s.n = *sine numero* (without a collecting number). Herbarium abbreviations are as follow: FHO = University of Oxford Herbarium , K = Royal Botanic Gardens Kew , ID, University of Idaho = Stillinger Herbarium , ANDES = Museo de Historia Natural Universidad de los Andes , WTU = University of Washington Herbarium , GH = Harvard University Herbarium , LJU = University of Ljubljana Herbarium , USFS = United States Forest Service , CBFS = University of South Bohemia České Budějovice. GenBank accessions for sequences not generated in this study are also shown.

Species	DNA Voucher/Herbarium	GenBank Accession Number				
		ITS	ETS	trnT-trnL	trnL-trnF	rps16
<i>Bartsia alpina</i> L.	Lampinen s.n/ID	FJ790046	KM408206	KM408239	KM434119	N/A
<i>B. crenoloba</i> Wedd.	Solomon 7152/K	KM408228	KM408185	KM408240	KM434106	KM408308
<i>B. laniflora</i> Benth.	SU-24/ANDES	KM408221	KM408174	KM408242	KM434110	KM408307
<i>B. laticrenata</i> Benth.	Ramsay & Merrow-Smith 771/K	KM408219	KM408178	KM408243	KM434104	N/A
<i>B. melampyroides</i> (Kunth) Benth.	Tank 2005-07/WTU	KM408218	KM408186	KM408245	KM434114	KM408300
<i>B. orthocarpiflora</i> Benth.	Ollgaard 34129/K	KM408216	KM408184	KM408246	KM434111	KM408296
<i>B. pedicularoides</i> Benth.	Jorgenson 1729/K	FJ790047	N/A	FJ790077	N/A	N/A
<i>B. pyricarpa</i> Molau	Tank 2005-36/WTU	KM408226	KM408182	KM408247	KM434102	KM408294
<i>B. ramosa</i> Molau	CG-016/ANDES	KM408229	KM408176	KM408248	KM434108	KM408304
<i>B. santolinifolia</i> (Kunth) Benth.	SU-18/ANDES	KM408220	KM408175	KM408249	KM434109	KM408306
<i>B. sericea</i> Molau	Tank 2005-06/WTU	KM408224	KM408181	KM408250	KM434105	KM408297
<i>B. cf sericea</i> Molau	Tank 2005-25/WTU	KM408227	KM408179	KM408251	KM434101	KM408302
<i>B. cf inaequalis</i> Benth. <i>ssp. duripilis</i> (Edwin) Molau	Tank 2005-29/WTU	KM408225	KM408183	KM408252	KM434107	KM408295
<i>B. stricta</i> (Kunth) Benth.	SU-1b/ANDES	KM408222	KM408177	KM408253	KM434112	KM408305
<i>B. tenuis</i> Molau	Tank 2005-02/WTU	KM408223	KM408180	KM408254	KM434103	KM408299
<i>B. thiantha</i> Diels	RGO 2009-23/WTU	KM408217	KM408187	KM408255	KM434113	KM408303

<i>Bellardia trixago</i> (L.) All.	Bennett s.n/FHO	FJ790063	KM408189	KM408256	KM434100	KM408301
<i>B. viscosa</i> (L.) Fisch. & C.A. Mey	Halse 2249/ID	AY911244	KM408188	KM408273	KM434095	KM408298
<i>Bornmuellerantha aucheri</i> (Boiss.) Rothm.	Oganesian et al. 03-1575/K	KM408237	KM408197	KM408267	KM434116	KM408279
<i>Euphrasia alsa</i> F.Muell.	Zich 220/GH	KM408212	KM408202	KM408257	KM434084	KM408282
<i>E. collina</i> R.Br.	Zich 209/GH	N/A	KM408203	KM408258	KM434086	KM408284
<i>E. mollis</i> (Ledeb.) Wettst.	Mancuso 107/ID	KM408213	N/A	KM408259	KM434082	KM408281
<i>E. regelii</i> Wettst.	Ho 1741/GH	KM408214	N/A	KM408260	KM434085	KM408285
<i>E. stricta</i> D. Wolff ex J.F. Lehm	Musselman 4872/ID	KM408215	N/A	KM408261	KM434098	KM408283
<i>Hedbergia abyssinica</i> (Benth.) Molau var. <i>abyssinica</i>	Etuge 3488/K	FJ790061	KM408194	KM408262	KM434120	KM408291
<i>H. abyssinica</i> (Benth.) Molau var. <i>nykiensis</i>	Carter et al 2386/K	KM408231	KM408193	KM408263	KM434122	N/A
<i>H. abyssinica</i> (Benth.) Molau var. <i>petitiana</i>	Paton s.n/K	KM408230	KM408195	KM408264	KM434123	KM408290
<i>H. decurva</i> (Hochst. ex Benth.) A. Fleischm. & Heubl	Wesche 9/K	N/A	KM408191	KM408241	KM434121	KM408292
<i>H. longiflora</i> ssp. <i>longiflora</i> (Hochst. ex Benth.) A. Fleischm. & Heubl	Kisalye van Heist 109/K	KM408232	KM408192	KM408244	KM434099	KM408286
<i>Lathraea squamaria</i> L.	Frajman s.n/LJU	FJ790044	KM408204	EU264174	KM434087	KM408309
<i>Melampyrum carstiense</i> Fritsch	Krajsek s.n/LJU	GU445314	N/A	EU264177	KM434088	KM408315
<i>M. lineare</i> Lam.	Bjork 6465/ID	KM408208	KM408207	KM408265	KM434096	KM408316
<i>M. sylvaticum</i> L.	Krajsek s.n/LJU	EU624134	N/A	KM408266	KM434089	KM408314
<i>Odontites corsicus</i> (Loisel.) G. Don	J. Stefani/ID	KM408238	KM408200	KM408268	KM434117	N/A
<i>O. linkii</i> Heldr. & Sart. ex Boiss. ssp. <i>cyprius</i>	Ferguson 4537/K	KM408234	KM408196	KM408269	KM434083	KM408288
<i>O. maroccanus</i> Bolliger	Gattefose s.n/K	KM408233	KM408198	KM408270	KM434097	N/A
<i>O. vulcanicus</i> Bolliger	Bolliger & Moser O-M3/K	KM408235	KM408199	KM408271	KM434115	KM408289
<i>O. vulgaris</i> Moench	Kharkevich s.n/K	KM408236	KM408201	KM408272	KM434118	KM408287
<i>Rhinanthus crista-galli</i> L.	Bjork 6656/ID	KM408210	N/A	KM408274	KM434091	KM408313
<i>R. freynii</i> (A.Kern. ex Sterneck) Fiori	Mathews 04-05	GU445319	KM408205	KM408275	KM434092	KM408310
<i>R. kyrollae</i> Chabert	Stickney 1236/USFS	KM408209	N/A	KM408276	KM434090	KM408312
<i>R. serotinus</i> (Schönh.) Oborny	Musselman 4871/ID	KM408211	N/A	KM408277	KM434093	KM408311
<i>Rhynchocorys elephas</i> Griseb.	Tesitel 5044/CBFS	FJ790055	N/A	FJ790085	N/A	N/A
<i>R. kurdica</i> Nábělek	Tesitel 5042/CBFS	FJ790037	N/A	FJ790067	N/A	N/A
<i>R. maxima</i> Richter	Tesitel 5040/CBFS	FJ790037	N/A	FJ790067	N/A	N/A
<i>R. odontophylla</i> R.B.Burbidge & I.Richardson	Tesitel 5038/CBFS	FJ790034	N/A	FJ790064	N/A	N/A
<i>R. orientalis</i> Benth.	Tesitel 5039/CBFS	FJ790035	N/A	FJ790065	N/A	N/A

<i>R. stricta</i> Albov	Tesitel 5047/ CBFS	FJ790057	N/A	FJ790087	N/A	N/A
<i>Tozzia alpina</i> L.	Mathews 04-04	AY911258	KM408190	KM408278	KM434094	KM408280

---

1 Table 2. Results for the Approximately Unbiased (AU) and the Shimodaira–Hasegawa (SH) tests  
 2 at  $p < 0.05$  for different constrained relationships. Log likelihood scores for the original analysis  
 3 are given, as well as the difference in log likelihood between the original and the constraint  
 4 topology ( $\hat{\delta}$ ). Values in bold are significant with 95% confidence.

5

nrDNA analysis constraint compared to clades from the	ln likelihood	$\hat{\delta}$	AU	SH
cpDNA analysis				
Unconstrained nrDNA analysis	-8445.56			
<i>Tozzia + Hedbergia</i>	-8449.04	3.48	0.166	0.186
<i>H. decurva + H. abyssinica</i> var. <i>nykiensis</i>	-8464.51	18.95	<b>0.004</b>	<b>0.026</b>
<i>Odontites + Bellardia</i>	-8456.43	10.87	0.141	0.131
cpDNA analysis constraint compared to clades from				
the nrDNA analysis				
Unconstrained cpDNA analysis	-10044.47			
<i>Tozzia + Bellardia</i>	-10064.45	19.98	<b>0.001</b>	<b>0.017</b>
<i>H. decurva + H. longiflora</i> ssp. <i>longiflora</i>	-10053.20	8.73	0.07	0.101
<i>Odontites + Euphrasia</i>	-10071.61	27.14	<b>0.0004</b>	<b>0.008</b>

6

7

8

9

10

11

12

13 Table 3. Divergence time estimates for the main clades, with each node representing the most  
14 recent common ancestor (mrca) of the taxa mentioned. The first value was obtained by  
15 calibrating the node of divergence of *Melampyrum* from its sister clade. The calibration point  
16 had a prior with lognormal distribution, offset 25 Myr, mean of 0.9, and standard deviation of  
17 0.8, using the results of Wolfe et al. (2005), but incorporating considerable temporal uncertainty.  
18 The second value corresponds to an additional analysis where the uplift of the Andes was used as  
19 the calibration point of the node of divergence for S. Am. *Bellardia*. This last calibration had a  
20 prior with a lognormal distribution, offset of 1.7 Myr, mean of 0.2, and standard deviation of 0.6.  
21 Median age estimates as well as the 95% highest posterior density (HPD) are shown for both  
22 analyses. In addition, the composite Akaike weights ( $w_i$ ) from our biogeographic analyses are  
23 shown for the ‘expert based’ coding of current geographic distributions with the following  
24 abbreviations: A (Africa), EU (Europe), EUR (Eurasia), ENA (Eastern North America), SAM  
25 (South America). Evidence ratio is presented for the most supported geographic reconstruction.

26

27

28

29

30

31

32

33

34

Node (mrca)	Median Age (Ma)	95% HPD (Ma)	$w_i$	Evidence Ratio	35
Root	30.65 / 30.98	25.55–38.83 / 29.13–35.96	EU 0.31	1.82	36
<i>Melampyrum</i>	14.70 / 15.02	7.41–24.89 / 7.14–24.32	EU 0.18	1.8	
<i>Lathraea–Bellardia</i>	27.01 / 27.38	25.19–31.64 / 20.87–33.57	EU 0.53	3.8	37
<i>Rhynchosorys–Lathraea</i>	20.53 / 20.33	15.18–26.27 / 13.97–26.88	EU 0.58	2.4	38
<i>Rhinanthus–Lathraea</i>	16.66 / 16.49	10.78–22.64 / 10.37–23.14	EU 0.53	2.2	
<i>Rhynchosorys</i>	11.65 / 11.57	7.13–17.43 / 6.69–17.45	EU 0.49	2.13	39
<i>Bartsia alpina–Bellardia</i>	22.62 / 22.33	17.49–28.07 / 16.23–28.36	EU 0.44	1.69	40
<i>Euphrasia–Bellardia</i>	19.25 / 19.02	14.35–24.23 / 13.72–24.60	EU+EUR 0.43	1.95	
<i>Euphrasia</i>	6.66 / 6.57	3.53–10.31 / 3.60–10.38	EUR 1.0	–	41
<i>Tozzia–Bellardia</i>	16.62 / 16.42	12.23–21.75 / 11.61–21.48	EU 0.53	1.76	42
<i>Tozzia–Hedbergia</i>	13.64 / 13.51	8.78–18.70 / 8.69–18.75	A+EU 0.94	23.5	
<i>H. longiflora–H. decurva</i>	6.94 / 6.90	3.67–10.93 / 3.60–10.96	A 0.99	247.5	43
<i>Odontites–Bellardia</i>	14.61 / 14.39	10.13–19.26 / 9.93–19.19	EU 0.80	8.88	
<i>Odontites</i>	9.38 / 9.29	6.22–13.02 / 5.94–13.29	EU 1.0	–	44
<i>Bellardia trixago–Neobartsia clade</i>	8.73 / 8.48	5.12–12.76 / 4.95–12.48	EU+SAM 0.26 EU 0.18 EU+EUR+SAM 0.16	1.44 1.13 –	45
<i>Bellardia viscosa–Neobartsia clade</i>	7.39 / 7.16	4.21–11.24 / 4.03–10.84	EU+SAM 0.53 EU+EUR+SAM 0.35 EUR+SAM 0.03	1.51 11.67 –	46
Neobartsia clade	2.59 / 2.63	1.51–4.08 / 1.97–3.58	SAM 1.0	–	47

48

49

50

51

52

53

54

55

56

57 Table 4. The composite Akaike weights ( $w_i$ ) are shown for our three different coding scenarios:  
 58 conservative, expert based, and species specific. Abbreviations are as follow: A (Africa), EU  
 59 (Europe), EUR (Eurasia), ENA (Eastern North America), SAM (South America). Evidence ratio  
 60 is presented for the most supported geographic reconstruction.  
 61

Coding Scheme	<i>Conservative</i>		<i>Expert based</i>		<i>Species specific</i>	
Node (mrca)	$w_i$	Evidence Ratio	$w_i$	Evidence Ratio	$w_i$	Evidence Ratio
Root	EU 0.52	3.71	EU 0.31	1.82	EU+ENA 0.40	1.05
<i>Melampyrum</i>	EU 0.25	3.57	EU 0.18	1.8	EU+ENA 0.93	4.65
<i>Lathraea–Bellardia</i>	EU 0.81	11.6	EU 0.53	3.8	EU 0.76	8.4
<i>Rhynchosorys–Lathraea</i>	EU 0.73	8.11	EU 0.58	2.4	EU 0.92	13.14
<i>Rhinanthus–Lathraea</i>	EU 0.67	6.1	EU 0.53	2.2	EU 0.96	13.7
<i>Rhynchosorys</i>	EU 0.62	5.16	EU 0.49	2.13	EU 0.70	2.59
<i>Bartsia alpina–Bellardia</i>	EU 0.84	16.8	EU 0.44	1.69	EU 0.59	3.10
<i>Euphrasia–Bellardia</i>	EU 0.80	26.6	EU+EUR 0.43	1.95	EU+EUR 0.40	1.81
<i>Euphrasia</i>	EU 0.26	2.88	EUR 1.0	–	EUR 1.0	–
<i>Tozzia–Bellardia</i>	EU 0.74	5.28	EU 0.53	1.76	EU 0.53	1.96
<i>Tozzia–Hedbergia</i>	A+EU 0.90	11.25	A+EU 0.94	23.5	A+EU 0.91	15.16
<i>Hedbergia</i>	A 0.98	122.5	A 0.99	247.5	A 0.98	81.66
<i>Odontites–Bellardia</i>	EU 0.79	26.03	EU 0.80	8.88	EU 0.76	7.6
<i>Odontites</i>	EU 0.74	6.16	EU 1.0	–	EU 0.93	15.5
<i>B. trixago–Neobartsia</i> clade	EU+SAM 0.21	1.31	EU+SAM 0.26	1.44	EU+SAM 0.24	1.33
	EU 0.16	1.45	EU 0.18	1.13	EU 0.18	1.06
	EU+EUR+SAM 0.11	–	EU+EUR+SAM 0.16	–	EU+EUR+SAM 0.17	–
<i>B. viscosa–Neobartsia</i> clade	EU+SAM 0.48	1.77	EU+SAM 0.53	1.51	EU+SAM 0.49	1.29
	EU+EUR+SAM 0.27	6.75	EU+EUR+SAM 0.35	11.67	EU+EUR+SAM 0.38	12.66
	EUR+SAM 0.04 SAM 1.0	–	EUR+SAM 0.03 SAM 1.0	–	EUR+SAM 0.03 SAM 1.0	–
Neobartsia clade	SAM 1.0	–	SAM 1.0	–	SAM 1.0	–

76

77

78

79

80 Table 5. Results from our diversification rate analyses using MEDUSA and SymmeTREE over a  
 81 posterior distribution of trees. The shifts were found at the nodes subtending the taxa specified in  
 82 the first column, followed by the frequency of that shift in the posterior distribution of trees, the  
 83 net diversification rate ( $r$ ) for the maximum clade credibility tree (mcc), and the mean, median,  
 84 minimum (min), maximum (max), and standard deviation (sd) summarized across 1,000 trees  
 85 from the posterior distribution. In the results for SymmeTREE, two different significance values  
 86 ( $\alpha$ ) were examined,  $\alpha < 0.05$ , and  $\alpha < 0.10$ .

87

88

<b>Node</b>	<b>Freq. shift</b>	<b><math>r</math> mcc</b>	<b><math>r</math> mean</b>	<b><math>r</math> median</b>	<b><math>r</math> min.</b>	<b><math>r</math> max.</b>	<b><math>r</math> sd</b>
<b>MEDUSA</b>							
<i>Bartsia alpina</i>	1.17	0	-0.04	-0.15	-0.32	0.33	0.18
<i>Tozzia-Hedbergia</i>	0.75	0.05	-0.06	0.00	-0.36	0.73	0.14
Neobartsia clade	0.40	0.79	0.40	0.38	0.15	1.03	0.13
Clade sister to <i>Bartsia alpina</i>	0.32	n/a	0.09	0.12	-0.18	0.26	0.07
<i>Rhinanthus-Lathraea</i>	0.12	n/a	0.17	0.16	0.12	0.28	0.03
<i>Core Rhinanthaeae</i>	0.07	n/a	0.11	0.12	-0.11	0.47	0.07

<b>SymmeTREE</b>	<b>Freq. shift at <math>p &lt; 0.05</math></b>	<b>Freq. shift <math>p &lt; 0.10</math></b>
<i>Bartsia alpina</i>	1.00	1.00
<i>Tozzia-Hedbergia</i>	0.00	0.93
Neobartsia clade	0.14	0.48

89

90

91

92

93

94

95



96 **Figure 1**

97 Majority rule consensus tree (excluding burn-in trees) with mean branch lengths from the  
98 partitioned Bayesian analysis of the combined dataset. Branch lengths are proportional to the  
99 number of substitutions per site as measured by the scale bar. Values above the branches  
100 represent Bayesian posterior probabilities (PP) and maximum likelihood bootstrap support (BS).  
101 Major clades are summarized following species names with the current species diversity in  
102 parenthesis.

103

104 **Figure 2**

105 Majority rule consensus tree (excluding burn-in trees) with mean branch lengths from the  
106 partitioned Bayesian analysis of the a) nuclear ribosomal (nr) DNA and b) the chloroplast (cp)  
107 DNA datasets. Branch lengths are proportional to the number of substitutions per site as  
108 measured by the scale bar. Values above the branches represent Bayesian posterior probabilities  
109 (PP) and maximum likelihood bootstrap support (BS).

110

111 **Figure 3**

112 Topology obtained after combining and annotating five independent BEAST analyses. The  
113 calibration point was set at the node where all genera are included except for *Melampyrum*. The  
114 calibration had a prior with a lognormal distribution, offset 25 Ma, a mean of 0.9, and a standard  
115 deviation of 0.8 following dates by Wolfe et al. (2005). Time in millions of years ago (Ma) is  
116 represented by the scale below the tree. Current distributions of the species are color-coded after  
117 the species names. The current distributions are plotted on a map below the species names and  
118 correspond to blue for Eurasia, red for Europe, yellow for Africa, black for northeastern North

119 America, and green for South America. The most supported ancestral range reconstructions  
120 obtained from a Lagrange analysis, are plotted on the tree with color rectangles or circles with  
121 numbers that represent different biogeographic hypotheses. Informally drawn ancestral range  
122 reconstruction scenarios are plotted on five different maps on the left of the figure, each with a  
123 number that distinguishes it. Composite Akaike weights ( $w_i$ ) are plotted in the form of  
124 histograms for nodes where the reconstruction had competing hypotheses. Two possible routes  
125 of migration, one including the North Atlantic Land Bridge (NALB) and one including the  
126 Bering Strait, are shown on maps 5 and 6.

127

128

129

130

131

132

133

134

135

136

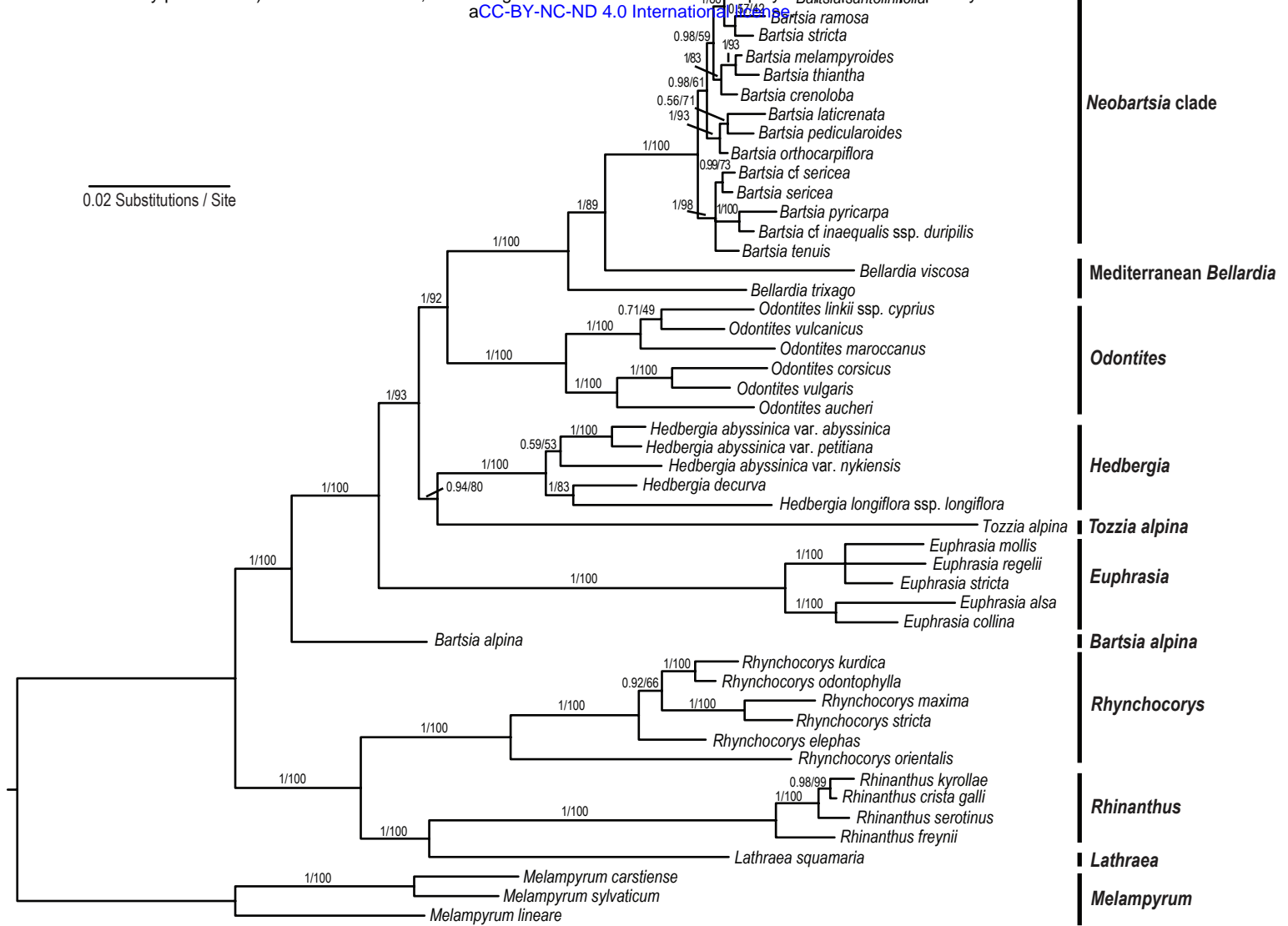
137

138

139

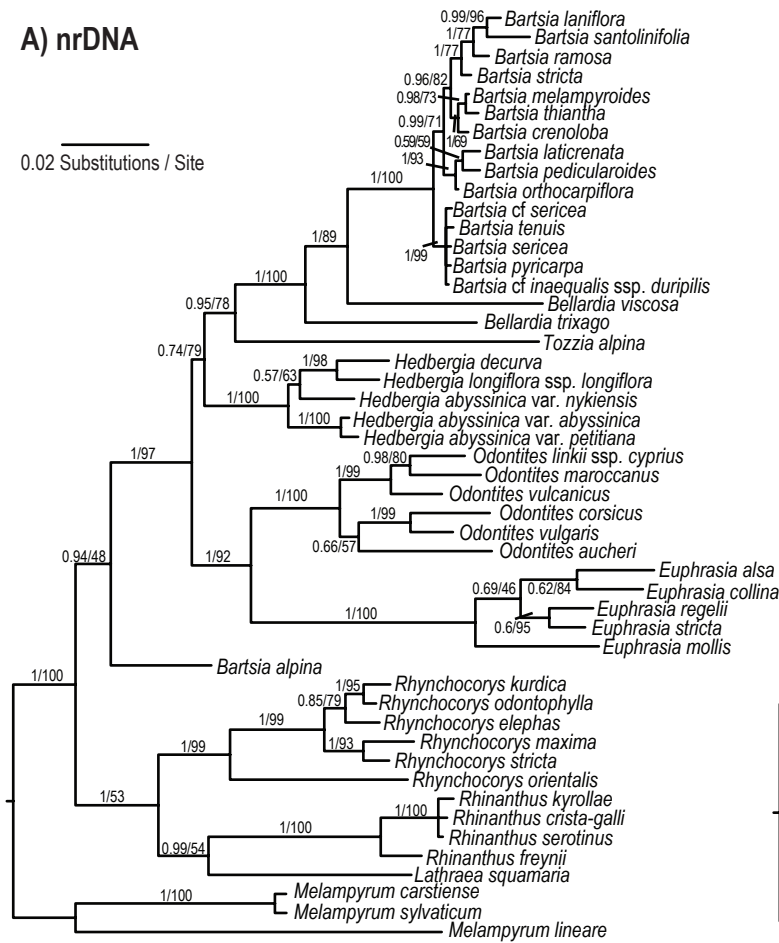
140

141



## A) nrDNA

0.02 Substitutions / Site



## B) cpDNA

